

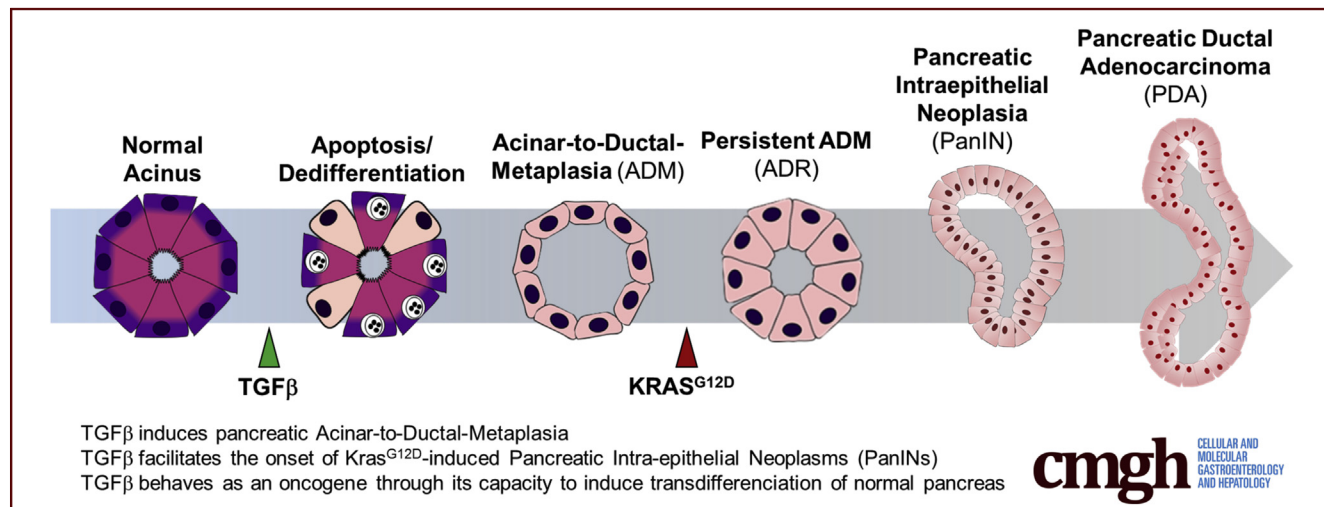
## ORIGINAL RESEARCH



# Acinar-to-Ductal Metaplasia Induced by Transforming Growth Factor Beta Facilitates KRAS<sup>G12D</sup>-driven Pancreatic Tumorigenesis

Nicolas Chuvin,<sup>1,a</sup> David F. Vincent,<sup>2,a</sup> Roxane M. Pommier,<sup>1</sup> Lindsay B. Alcaraz,<sup>1</sup> Johann Gout,<sup>1</sup> Cassandre Caligaris,<sup>1</sup> Karam Yacoub,<sup>1</sup> Victoire Cardot,<sup>1</sup> Elodie Roger,<sup>1</sup> Bastien Kaniewski,<sup>1</sup> Sylvie Martel,<sup>1</sup> Celia Cintas,<sup>3</sup> Sophie Goddard-Léon,<sup>1</sup> Amélie Colombe,<sup>1</sup> Julie Valantin,<sup>4</sup> Nicolas Gadot,<sup>4</sup> Emilie Servoz,<sup>5</sup> Jennifer Morton,<sup>2</sup> Isabelle Goddard,<sup>5</sup> Anne Couvelard,<sup>6,7,8</sup> Vinciane Rebours,<sup>9</sup> Julie Guillermet,<sup>3</sup> Owen J. Sansom,<sup>2</sup> Isabelle Treilleux,<sup>4</sup> Ulrich Valcourt,<sup>1</sup> Stéphanie Sentis,<sup>1</sup> Pierre Dubus,<sup>10,11</sup> and Laurent Bartholin<sup>1</sup>

<sup>1</sup>Université de Lyon, Université Claude Bernard Lyon 1, Inserm 1052, CNRS 5286, Centre Léon Bérard, Centre de Recherche en Cancérologie de Lyon (CRCL), Lyon, France; <sup>2</sup>Cancer Research UK Beatson Institute, Institute of Cancer Sciences, University of Glasgow, Glasgow, United Kingdom; <sup>3</sup>Inserm U1037, Université Toulouse III, Centre de Recherches en Cancérologie de Toulouse (CRCT), Oncopole de Toulouse, Toulouse, France; <sup>4</sup>Plateforme Anatomopathologie Recherche, Département de Recherche Translationnelle et de l'Innovation, Centre Léon Bérard, Lyon, France; <sup>5</sup>Département de Recherche Translationnelle et de l'Innovation, Centre de Recherche en Cancérologie de Lyon (CRCL), Inserm U1052-CNRS UMR5286, Université de Lyon Centre Léon Bérard, Laboratoire des Modèles Tumoraux (LMT) Fondation Synergie Lyon Cancer, Lyon, France; <sup>6</sup>Inserm U1149, Faculté de Médecine Xavier Bichat, Paris, France; <sup>7</sup>Université Denis Diderot-Paris 7, Paris, France; <sup>8</sup>AP-HP, DHU UNITY, Hôpital Bichat, Département de Pathologie Beaujon-Bichat, Paris, France; <sup>9</sup>Pancreatology Unit, DHU UNITY, Beaujon Hospital, APHP; Inserm - UMR 1149, University Paris 7, Paris, France; <sup>10</sup>Université Bordeaux, Inserm U1053, Bordeaux, France; and <sup>11</sup>CHU Bordeaux, Bordeaux France



## SUMMARY

Acinar-to-Ductal Metaplasia (ADM) is considered the main origin of pancreatic pre-neoplastic lesions that eventually develop into Pancreatic Ductal Adenocarcinoma (PDA). ADM could be a decisive step during tumorigenesis, selecting plastic cells for a more aggressive subsequent tumorigenesis. Our results indicate that TGF $\beta$ , a cytokine overexpressed during early and late pancreatic tumorigenesis, is an inducer of ADM and set up a favorable context for the emergence of oncogene-driven neoplastic lesions. This questions the usual dichotomist vision of TGF $\beta$  in PDA.

**BACKGROUND & AIM:** Transforming growth factor beta (TGF $\beta$ ) acts either as a tumor suppressor or as an oncogene, depending on the cellular context and time of activation. TGF $\beta$  activates the canonical SMAD pathway through its interaction with the serine/threonine kinase type I and II heterotetrameric receptors. Previous studies investigating TGF $\beta$ -mediated signaling in the pancreas relied either on loss-of-function approaches or on ligand overexpression, and its effects on acinar cells have so far remained elusive.

**METHODS:** We developed a transgenic mouse model allowing tamoxifen-inducible and Cre-mediated conditional activation of

a constitutively active type I TGF $\beta$  receptor (T $\beta$ RI $^{CA}$ ) in the pancreatic acinar compartment.

**RESULTS:** We observed that T $\beta$ RI $^{CA}$  expression induced acinar-to-ductal metaplasia (ADM) reprogramming, eventually facilitating the onset of KRAS $^{G12D}$ -induced pre-cancerous pancreatic intraepithelial neoplasia. This phenotype was characterized by the cellular activation of apoptosis and dedifferentiation, two hallmarks of ADM, whereas at the molecular level, we evidenced a modulation in the expression of transcription factors such as *Hnf1 $\beta$* , *Sox9*, and *Hes1*.

**CONCLUSIONS:** We demonstrate that TGF $\beta$  pathway activation plays a crucial role in pancreatic tumor initiation through its capacity to induce ADM, providing a favorable environment for KRAS $^{G12D}$ -dependent carcinogenesis. Such findings are highly relevant for the development of early detection markers and of potentially novel treatments for pancreatic cancer patients. (*Cell Mol Gastroenterol Hepatol* 2017;4:263–282; <http://dx.doi.org/10.1016/j.jcmgh.2017.05.005>)

**Keywords:** Pancreas; Cancer; TGF $\beta$ ; Acinar-to-Ductal Metaplasia; KRAS $^{G12D}$ .

In mammals, the pancreas is a bifunctional organ.<sup>1</sup> The exocrine pancreas, composed of acinar cells and ducts, accounts for more than 90% of the organ's mass. Acinar cells secrete digestive enzymes that are further collected in a network of ducts that discharge pancreatic juices into the duodenum. The endocrine tissue, represented by islets of Langerhans embedded in the exocrine pancreas, controls blood glucose levels by secreting hormones such as insulin and glucagon. Embryonically, all pancreatic lineages arise from a multipotent progenitor present at day E9 in the mouse endoderm.<sup>2</sup> The fate of the pancreas is dictated by the expression of progenitor markers such as SOX9 and CK19 for ductal cells, MIST1, PTF1A, CPA1, and ELA1 for acinar cells, and NGN3 for endocrine cells.<sup>2–4</sup> Note that PTF1A is required for the specification of the pancreatic multipotent progenitor cells and is later expressed only in the adult acinar compartment.<sup>5</sup>

The adult pancreas is highly plastic<sup>6</sup> to ensure organ integrity in response to internal (intracellular activation of digestive enzymes, obstruction of main ducts potentially as a result of gallstones) or external stresses (alcohol, trauma). Repair and regeneration of the injured organ are orchestrated by many cell types including acinar cells, centroacinar cells, ductal cells, immune cells, and stellate cells.<sup>7,8</sup> The existence of a resident stem cell population in the organ remains controversial.<sup>9,10</sup> Many studies<sup>1,11,12</sup> have focused on post-injury pancreatic regeneration and demonstrated the crucial role of acinar cells during this process. Indeed, under severe stress conditions such as pancreatitis, acinar cells undergo acinar-to-ductal metaplasia (ADM), a morphologic and transcriptional conversion into duct-like cells with embryonic progenitor cell properties.<sup>5,7,13</sup> These metaplastic cells are then capable of proliferating to replenish the damaged organ. In the case of a sustained stress signal or concomitant oncogenic activation such as

KRAS activating mutations (eg, KRAS $^{G12D}$ ), the metaplastic cells cannot revert to a differentiated state, as generally observed in the case of an acute stress. This pancreatic erosion process constitutes a favorable setting for the onset of low-grade pancreatic intraepithelial neoplasia (PanIN).<sup>14</sup> Progression toward PanINs of higher grade and eventually pancreatic ductal adenocarcinoma (PDA) is associated with recurrent mutations or genetic/epigenetic alterations in tumor suppressor genes (*INK4/ARF*, *TP53*).<sup>15,16</sup> Importantly, SMAD4/DPC4, a core component of the transforming growth factor beta (TGF $\beta$ ) signaling pathway, is deleted in 50% of PDAs.<sup>16–18</sup> Members of the TGF $\beta$  superfamily of transforming growth factors are involved in embryonic development, regulation of homeostasis, and the pathogenesis of a variety of diseases.<sup>19,20</sup> TGF $\beta$  signaling occurs through a heterotetrameric receptor complex composed of 2 subunits, the type I and type II TGF $\beta$  receptors (T $\beta$ RI and T $\beta$ RII, respectively). On binding to its receptors, TGF $\beta$  enables T $\beta$ RII to transphosphorylate T $\beta$ RI, which in turn activates the canonical SMAD pathway (phosphorylation of SMAD2 and SMAD3 that further interact with SMAD4 to accumulate inside the nucleus) and other signaling pathways (MAPK, RHOA, and PI3K/AKT).<sup>21</sup> In cancer, TGF $\beta$  behaves as either a tumor suppressor or a tumor promoter. Indeed, TGF $\beta$  is generally considered to be a tumor suppressor early in tumor development (tumor initiation) by restricting epithelial cell growth (through cytostasis and apoptosis).<sup>19,22,23</sup> However, in later stages of tumorigenesis (tumor progression), TGF $\beta$  has oncogenic properties through its capacity to regulate cellular plasticity by stimulating biological processes, including extracellular matrix deposition, immune evasion, epithelial-to-mesenchymal transition (EMT), and stemness.<sup>22,24–27</sup>

Unlike the majority of previously published studies in which the TGF $\beta$  signaling pathway was abrogated, our present work addresses the consequences of TGF $\beta$  cell-autonomous activation in the pancreatic epithelial lineage. To this end, we generated a unique mouse model enabling us to express a constitutively activated T $\beta$ RI receptor (T $\beta$ RI $^{CA}$ ) exclusively in pancreatic acinar cells, starting either in the embryo or after birth. Hence, we demonstrate that the specific activation of TGF $\beta$  signaling in pancreatic acinar cells induced ADM reprogramming and eventually facilitated the onset of KRAS $^{G12D}$ -induced PanINs and PDA progression.

<sup>a</sup>Authors share co-first authorship.

**Abbreviations used in this paper:** ADM, acinar-to-ductal metaplasia; AFI, acinar fatty infiltration; EMT, epithelial-to-mesenchymal transition; PanIN, pancreatic intraepithelial neoplasia; PBS, phosphate-buffered saline; PDA, pancreatic ductal adenocarcinoma; RT-qPCR, reverse transcription quantitative polymerase chain reaction; TGF $\beta$ , transforming growth factor beta; TUNEL, terminal deoxynucleotidyl transferase dUTP nick end labeling.

 Most current article

© 2017 The Authors. Published by Elsevier Inc. on behalf of the AGA Institute. This is an open access article under the CC BY-NC-ND license (<http://creativecommons.org/licenses/by-nc-nd/4.0/>).

2352-345X

<http://dx.doi.org/10.1016/j.jcmgh.2017.05.005>

## Materials and Methods

### Mouse Strains and Handling

The *LSL-T $\beta$ RI<sup>CA</sup>* strain was previously generated in the laboratory of Dr Bartholin<sup>28,29</sup> (*T $\beta$ RI<sup>CA</sup>* is tagged with the hemagglutinin epitope at the C-terminus). We and others have functionally validated the *T $\beta$ RI<sup>CA</sup>* transgene after successful in vivo targeting in different subcellular compartments or organs such as immune cells,<sup>28,30–35</sup> ovaries,<sup>36</sup> and uterine tissue.<sup>37</sup> In the present study, we only used *T $\beta$ RI<sup>CA</sup>* males to circumvent the mosaic phenotype occurring in females as a result of random X chromosome inactivation and associated inactivation of the transgene in a proportion of cells, as previously reported for other transgenes located on the X chromosome.<sup>38</sup> *LSL-Kras<sup>G12D</sup>*<sup>39</sup>, *Pdx1-Cre*,<sup>40</sup> *Ptf1a-Cre<sup>ERT2</sup>*<sup>5</sup>, and *Rosa-Cre<sup>ERT2</sup>*<sup>41</sup> alleles have been described previously. *E2A-Cre*<sup>42</sup> allele has been described previously; [*E2A-Cre*<sup>+/+</sup>] or [*E2A-Cre*<sup>+/-</sup>] mice were crossed with [*LSL-T $\beta$ RI<sup>CA</sup>*] (R) mice.

19.5 embryos were removed from [*LSL-T $\beta$ RI<sup>CA</sup>*] females (R) previously impregnated by [*Pdx1-Cre*] males (C). To this end, pregnant females (R; n = 11) were euthanized at 19.5 days *post coitum*, and embryos were collected (n = 92).

Five-week-old mice bearing the *Ptf1a-Cre<sup>ERT2</sup>* allele along with *LSL-T $\beta$ RI<sup>CA</sup>* and/or *LSL-Kras<sup>G12D</sup>* transgenes were injected with tamoxifen (Sigma-Aldrich #T5648; St Louis, MO; 3 mg per injection) to induce recombination of the *LSL-T $\beta$ RI<sup>CA</sup>* and *LSL-Kras<sup>G12D</sup>* alleles. Animals from the 3-day cohort received 2 injections (day 1 and day 3) and were killed at day 4. Animals from the 3-week, 2-month, and 6-month cohorts received 5 injections (days 1, 3, 5, 7, and 9) and were killed 3 weeks, 2 months, and 6 months after the first injection, respectively. For *Rosa26-Cre<sup>ERT2</sup>* mice, tamoxifen was injected 7-10 weeks after birth.

Mice were housed and bred in the AniCan specific pathogen-free animal facility of the Centre de Recherche en Cancérologie de Lyon, France. The experiments were performed in compliance with the animal welfare guidelines of the European Union and with French legislation (CECCAPP protocol #CLB-2014-008).

### Histology and Immunohistochemistry/

#### Immunofluorescence

Histologic (H&E staining) and immunohistochemical experiments were performed as described previously.<sup>43,44</sup> For immunohistochemistry experiments, the primary antibodies used were anti-CK19 (Developmental Studies Hybridoma Bank, Iowa City, IA) and anti-INSULIN (Dako A0564; Glostrup, Denmark). The secondary antibodies used were rat immunoglobulin G (H+L) biotinylated (Vector #BA-9400; Vector Laboratories, Burlingame, CA) and guinea pig immunoglobulin G (H+L) biotinylated (Vector #BA-7000). For AMYLASE/CK19 double immunofluorescence, primary antibodies were anti-AMYLASE (Sigma-Aldrich A8273) and anti-CK19 (Developmental Studies Hybridoma Bank) and secondary antibodies used were Rabbit IgG (H+L) Alexa Fluor 647-conjugated (Life Technologies #A-21245 GAR647) and Rat IgG (H+L) Alexa Fluor

594-conjugated (Life Technologies #A-21209 DAR594). For AMYLASE/SOX9 double immunofluorescence, primary antibodies were anti-AMYLASE (Santa-Cruz #166349), anti-SOX9 (Millipore #AB5535) and secondary antibodies used were Rabbit IgG (H+L) Alexa Fluor 647-conjugated (Life Technologies #A-21245 GAR647) and Mouse IgG (H+L) Alexa Fluor 488-conjugated (Life Technologies #A-11001 GAM488), but artificial colors (red for AMYLASE and green for SOX9) were given with the Zeiss software to be consistent with AMYLASE/CK19 double staining. Nuclei were counterstained with DAPI, and images were acquired with a Zeiss Imager M2 AX10 (Carl Zeiss AG, Oberkochen, Germany).

### Quantification of Pancreatic Lesions

Histologic scoring of pancreatic lesions was performed by using 1 representative H&E tissue slide per animal (3–8 animals per condition). Pancreatic lesions were scored from PanIN1 to PanIN3/PDA and were counted. The area of the analyzed tissue was determined by using ImageJ software (National Institutes of Health, Bethesda, MD), and lesion counts were normalized to this area.

### RNAscope

*T $\beta$ RI<sup>CA</sup>* mRNA and *Smad7* mRNA were detected *in situ* by using the RNAscope technology (Advanced Cell Diagnostics, Newark, CA) for the *Hu-T $\beta$ RI* (catalog no. 431041) and *Mm-Smad7* (catalog no. 429411) probes, respectively.

### Cell Culture

The rat pancreatic acinar cell line AR42J (ATCC) was cultured in Dulbecco modified Eagle medium supplemented with fetal calf serum (Lonza Group, Basel, Switzerland) and penicillin/streptomycin (Gibco Laboratories, Gaithersburg, MD). AR42J cells were infected with murine retroviral particles containing a wild-type (*pZip-Neo*) vector or a KRAS<sup>G12D</sup>-expressing vector (*pZIP-Neo-KRAS<sup>G12D</sup>*; donated by Dr J. Caramel, CRCL, Lyon, France) and further cultured in the presence of Geneticin (PAA Laboratories, Linz, Austria). TGF $\beta$  was used at the final concentration of 10 ng/mL.

For proliferation assays, AR42J-WT and AR42J-KRAS<sup>G12D</sup> were seeded in triplicate at 100,000 cells per well onto 12-well plates and treated with TGF $\beta$  (10 ng/mL; PeproTech #100-21; Rocky Hill, NJ) for 24 and 48 hours. For each time point, cells were morphologically examined by phase-contrast microscopy and counted by using the trypan blue exclusion method. Kinase inhibitors were used as follows: 5  $\mu$ mol/L T $\beta$ RI inhibitor (SB 431542, Sigma-Aldrich #S4317), 10  $\mu$ mol/L MEK inhibitor (U0126 monoethanolate, Sigma-Aldrich #U120), 2.5  $\mu$ mol/L JNK inhibitor (Selleckchem #S4901; Houston, TX), 2.5  $\mu$ mol/L PI3K inhibitor (LY294002, Selleckchem #S1105), and 2.5  $\mu$ mol/L p38 inhibitor (SB 203580; Enzo Life Sciences, Farmingdale, NY; #BML-EI286-0001). Inhibitors

were added 1 hour before TGF $\beta$  treatment (10 ng/mL) and maintained during the 48 hours of TGF $\beta$  treatment.

### Immunoprecipitation

For protein analysis, mouse pancreas tissue was lysed and homogenized in RIPA buffer (50 mmol/L Tris-HCl pH 7.4, 150 mmol/L NaCl, 1 mmol/L ethylenediamine tetraacetic acid, 0.5% sodium deoxycholate, 0.1% sodium dodecylsulfate, and 1% Nonidet) containing a cocktail of protease and phosphatase inhibitors. After protein quantification, 40  $\mu$ g protein was used for loading controls, and 2.5 mg protein was used for the immunoprecipitation assay by using the SMAD2/3 antibody (Cell Signaling Technology #3102; Danvers, MA) and protein G Agarose Fast Flow (EMD Millipore). Proteins were separated by sodium dodecylsulfate-polyacrylamide gel electrophoresis and detected by Western blot analysis.

### Western Blot Analysis

Western blotting was performed as previously described.<sup>29</sup> The primary antibodies used were anti-phospho-SMAD2 (Cell Signaling #3101), anti-SMAD2 (Invitrogen #51-1300; Carlsbad, CA), anti-SMAD2/3 (Cell Signaling #3102), anti-SMAD4 (Epitomics #1676-1; Burlingame, CA), anti-RAS (Santa Cruz Biotechnology), anti- $\beta$ -actin (Sigma-Aldrich #A5441 Clone AC15), and anti- $\beta$ -tubulin (mouse monoclonal; Sigma-Aldrich). Peroxidase-labeled anti-rabbit and anti-mouse secondary antibodies were purchased from Dako (mouse immunoglobulin G horseradish peroxidase-conjugated DAKO P0260, rabbit immunoglobulin G horseradish peroxidase-conjugated DAKO #P0448).

### Polymerase Chain Reaction and Reverse Transcription Quantitative Polymerase Chain Reaction

PCR to detect the recombined  $T\beta R^{CA}$  allele was performed as described previously.<sup>28</sup>

AR42J-WT and AR42J-KRAS<sup>G12D</sup> were treated for 48 hours with 10 ng/mL TGF $\beta$  (PreproTech #100-21) before being washed with phosphate-buffered saline (PBS). RNA extraction was performed by using the RNeasy mini kit (QIAGEN #74104; Hilden, Germany), according to the manufacturer's instructions.

For pancreatic tissues, RNA extraction from frozen tissue was performed by using guanidine thiocyanate enriched lysis solution containing 5 mol/L guanidine thiocyanate (Sigma-Aldrich #G6639), 2.5 mmol/L sodium citrate, 0.5% N-lauryl sarcosine (Sigma-Aldrich #61739), and 1%  $\beta$ -mercaptoethanol. Lysates were centrifuged at 14,000 rpm at 4°C for 5 minutes to eliminate cell fragments. RNA was consecutively purified with the RNeasy mini kit (QIAGEN #74104), according to the manufacturer's instructions.

After RT (ThermoFisher Scientific, Waltham, MA) by using random primers, qPCR was performed by using the MESA GREEN qPCR MasterMix Plus for SYBR Assay ROX

(Eurogentec, Liège, Belgium; #RT-SY2X-06+WOU) and the following primers:

<i>Ela1</i> :	Forward: 5'-TGGTCCTGTATGGACACAGT-3' Reverse: 5'-CCGTCATTCTGACTCAGGGT-3'
<i>Mist1</i> :	Forward: 5'- TGGCTAAAGCGACGTGTC-3' Reverse: 5'- CTTCCGACTGGGGATCCGA-3'
<i>Cpa1</i> :	Forward: 5' - ACTTTGTGGGACACCAGGT-3' Reverse: 5' - ACATCAATGGGGATACCGGC-3'
<i>Sox9</i> :	Forward: 5'- GTGCTGAAGGGCTACGACTGGA-3' Reverse: 5'- GTTGTGCAGATGCGGGTACTGG-3'
<i>Hnf1<math>\beta</math></i> :	Forward: 5'- TCCCACATCTGCAATGGTGGTC-3' Reverse: 5'- GCTGTGCACAAAGTGAGTGG-3'
<i>Hes1</i> :	Forward: 5'- GTCCCCGGTGGCTGCTAC-3' Reverse: 5'- AACACGCTGGGTCTGTGCT-3'
<i>Serpine-1</i> :	Forward: 5'- CCCACGGAGATGGTTAG -3' Reverse: 5'- ATCACTTGGCCATGAAGAG -3'
<i>T<math>\beta</math>R<sup>CA</sup></i> :	Forward: 5'- TTGTGAACAGAACAGTTAAGGC -3' Reverse: 5'- AGCATAATCAGGAACATCAT -3'
<i>Actb</i> :	Forward: 5'- GCAGGAGTACGATGAGTCCG-3' Reverse: 5'- ACGCAGCTCAGTAACAGTCC-3'
<i>Bmf</i> :	Forward: 5'- AGGTACAGATGCCAGAAAGC-3' Reverse: 5'- CTCGGTTCTGCTGGTGTGTTG-3'

### RAS Activity Assay

GTP-bound RAS (activated RAS) was measured in cell lysates incubated with beads coated with RAF1-RBD (Upstate; EMD Millipore). The experiment was performed by using the active RAS detection kit (Cell Signaling Technology #8821).

### Cell Death Assays

For the caspase-3 activity assay, AR42J-WT and AR42J-KRAS<sup>G12D</sup> cells were treated with 10 ng/mL TGF $\beta$  for 12 hours. Caspase-3 activity was determined by using the CASPASE-3/CPP32 Fluorimetric Assay Kit, according to the manufacturer's instructions (Gentaur Biovision, Kampenhout, Belgium). For the annexin V assay, AR42J-WT and AR42J-KRAS<sup>G12D</sup> cells were seeded in duplicate and treated with 10 ng/mL TGF $\beta$  for 48 hours (PeproTech). Cells were harvested in PBS and incubated with annexin V-fluorescein isothiocyanate and propidium iodide (BD Pharmingen, San Diego, CA), according to the manufacturer's instructions, and analyzed by flow cytometry (FACS Calibur cytometer; BD Biosciences). For the TUNEL cell death assay, AR42J-WT and AR42J-KRAS<sup>G12D</sup> (24 hours of TGF $\beta$  treatment) cells or tissue sections were fixed in formaldehyde before being permeabilized with PBS-0.2% Triton X-100 and incubated in TdT buffer, 1 mmol/L CoCl<sub>2</sub> (Sigma-Aldrich # 15862-1 mL-F) for 5 minutes. Then they were incubated with TdT buffer (30 mmol/L Tris, 150 mmol/L sodium cacodylate, pH7.5), 1 mmol/L CoCl<sub>2</sub>, Biotin16-dUTP (Sigma-Aldrich #11093070910), TdT enzyme (Roche #11767305001; Basel, Switzerland) for 1 hour at 37°C. The reaction was

stopped by incubating the samples with 300 mmol/L NaCl, 2.5 mmol/L sodium citrate for 15 minutes. After washing with PBS, unspecific sites were saturated with 2% bovine serum albumin, 10 mmol/L PBS. After washing with PBS, slides were incubated with streptavidin-Cy3 (Jackson ImmunoResearch, West Grove, PA) diluted 1/200 in 2% bovine serum albumin in PBS. Finally, the nuclei were counterstained with DAPI (Sigma-Aldrich), and images were acquired with a Zeiss Imager M2 AX10.

## Results

### Transforming Growth Factor Beta-induced Cell Growth Inhibition In Vitro Is Enhanced in Acinar Cells Expressing KRAS<sup>G12D</sup>

We initially explored the combined effects of KRAS activation and TGF $\beta$  treatment on rat AR42J pancreatic acinar cells<sup>45,46</sup> infected either with a wild-type retroviral vector (AR42J-WT cells) or with a KRAS<sup>G12D</sup> retroviral vector (AR42J-KRAS<sup>G12D</sup> cells). We ascertained that KRAS<sup>G12D</sup> was present and functional in AR42J-KRAS<sup>G12D</sup> cells via Western blot analysis, which revealed a significant increase in the level of active GTP-bound RAS protein compared with AR42J-WT cells (Figure 1A). Examination of the cells by phase-contrast microscopy revealed that AR42J-KRAS<sup>G12D</sup> cells treated with TGF $\beta$  grew to a lower cell density than the other cell populations (Figure 1B). This growth-inhibition effect was confirmed by counting cells, highlighting a clear decrease in the number of AR42J-KRAS<sup>G12D</sup> cells treated with TGF $\beta$  (Figure 1C). Furthermore, this decrease was much stronger than that observed for AR42J-WT cells. Functionally, although these latter cells were poorly responsive to TGF $\beta$  with respect to their capacity to phosphorylate SMAD2 (P-SMAD2), AR42J-KRAS<sup>G12D</sup> cells displayed a drastic increase in P-SMAD2 on TGF $\beta$  treatment, as evidenced by Western blot analysis (Figure 1D). As expected, the levels of SMAD2/3 and SMAD4 were affected neither by KRAS activation nor by TGF $\beta$  treatment. Taken together, these results demonstrate that the activation of KRAS potentiates TGF $\beta$  cell growth inhibition and SMAD pathway activation in rat pancreatic acinar cells.

### KRAS<sup>G12D</sup> Sensitizes Acinar Cells to Transforming Growth Factor Beta-induced Apoptosis and Dedifferentiation In Vitro

Next, we speculated that the inhibition of AR42J-KRAS<sup>G12D</sup> pancreatic acinar cell growth in the presence of TGF $\beta$  was due to apoptosis.<sup>47</sup> Microscopic examinations revealed that TGF $\beta$ -treated AR42J-KRAS<sup>G12D</sup> cells were characterized by the presence of poorly refringent cells (Figure 1B, inset) and by an increase in the number of floating cells (data not shown), evoking the presence of apoptotic cells. The highest rates of apoptosis were observed in AR42J-KRAS<sup>G12D</sup> cells treated with TGF $\beta$ , as demonstrated by caspase-3 activity (Figure 2A), terminal deoxynucleotidyl transferase dUTP nick end labeling (TUNEL) (Figure 2B), and annexin-V (Figure 2C) assays. TGF $\beta$ -induced apoptosis mainly occurs via the mitochondrial pathway by downregulating antiapoptotic factors of the BCL-2 family (BCL-xL) and by positively regulating proapoptotic

factors of the BCL-2 family.<sup>23</sup> Proapoptotic *Bmf* (BCL2-modifying factor) was previously shown to be upregulated after TGF $\beta$  treatment in the normal murine mammary epithelial cell line NMuMG.<sup>48</sup> Reverse transcription quantitative polymerase chain reaction (RT-qPCR) experiments performed on total RNA prepared from AR42J-WT and AR42J-KRAS<sup>G12D</sup> cells showed an increase of *Bmf* mRNA expression after TGF $\beta$  treatment (Figure 2D). This activation is compromised in the presence of SB431542, an inhibitor of T $\beta$ RI kinase activity. These observations are consistent with the increase in apoptosis observed by caspase-3, TUNEL, and annexin-V assays.

Phase-contrast micrographs revealed that TGF $\beta$ -treated AR42J-KRAS<sup>G12D</sup> cells (and to a lesser extent AR42J-WT cells) acquired a spindle-like shape after TGF $\beta$  treatment (Figure 3A). RT-qPCR did not reveal significant changes in response to TGF $\beta$  in EMT markers such as *Sna1*, *Zeb1*, *Vimentin*, and *Cdh2* in AR42J-WT and AR42J-KRAS<sup>G12D</sup> cells (data not shown). In contrast, a decrease in the expression of acinar markers (*Ela1*, *Cpa1*, and *Mist1*) and a marked increase in the expression of ductal/dedifferentiation/progenitor markers (*Hes1*, *Hnf1 $\beta$* , *Sox9*) were observed in AR42J-KRAS<sup>G12D</sup> cells treated with TGF $\beta$  (Figure 3B). These morphologic and transcriptional changes are reminiscent of ADM. Among the genes we tested and known to be positively correlated to ADM, we focused our interest on *Hnf1 $\beta$*  because it was the best TGF $\beta$  responder in experiments presented in Figure 3B. TGF $\beta$  signaling is mediated by both the canonical SMAD pathway and non-canonical pathways (MAPK, PI3K, RHO-RAC).<sup>22,23</sup> AR42J-WT cells were cultured in the presence of TGF $\beta$  along with kinase inhibitors of both the canonical and non-canonical TGF $\beta$  pathways. RT-qPCR revealed that *Hnf1 $\beta$*  activation depends on SMAD and MEK pathways but not on JNK, P38, or PI3K pathways (Figure 3C).

These results demonstrate that TGF $\beta$  treatment and KRAS activation cooperate to compromise AR42J rat acinar cell differentiation by increasing both apoptosis and ductal-like reprogramming, two hallmarks of ADM *in vivo*.

### Activation of Transforming Growth Factor Beta Signaling in the Mouse Embryonic Pancreas Severely Compromises the Development of the Acinar Compartment

We then analyzed whether the activation of TGF $\beta$  signaling (alone or in combination with KRAS activation) could compromise the homeostasis of pancreatic acinar cells *in vivo*. To achieve this, we used a mouse strain ([*LSL-T $\beta$ RI*<sup>CA</sup>] also called R) containing a constitutively active TGF $\beta$  type I receptor (T $\beta$ RI), previously generated in the laboratory of Dr Bartholin by using a knock-in strategy.<sup>28,30</sup> Transgene expression under the control of the ubiquitous *CAG* (human cytomegalovirus enhancer and chicken  $\beta$ -actin) promoter is repressed by a floxed transcriptional Stop (*Lsl, Lox-Stop-Lox*), which can be excised in the presence of Cre recombinase. *E2A-Cre* allows recombination early during embryonic development before the E5 uterine wall implantation stage. We never

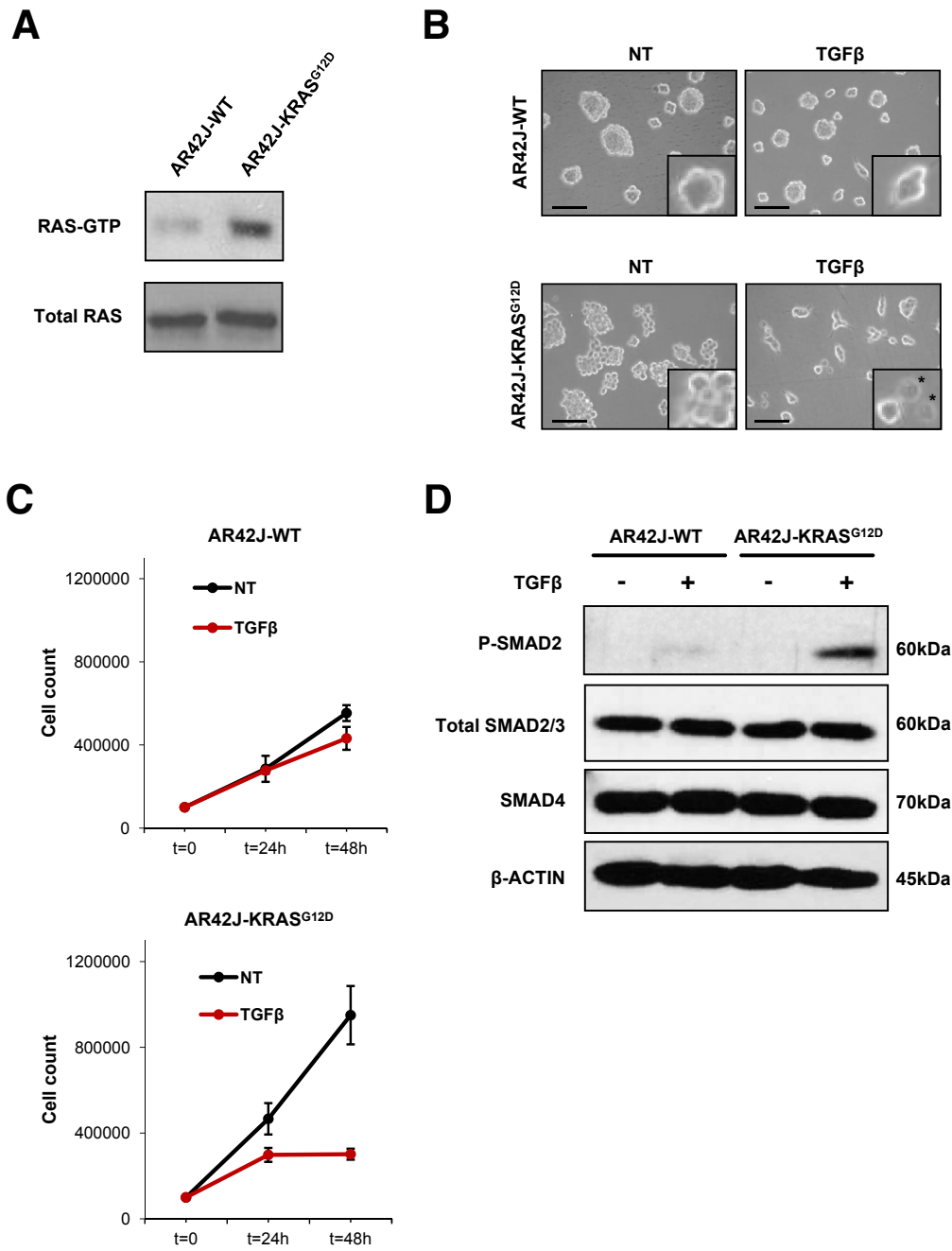
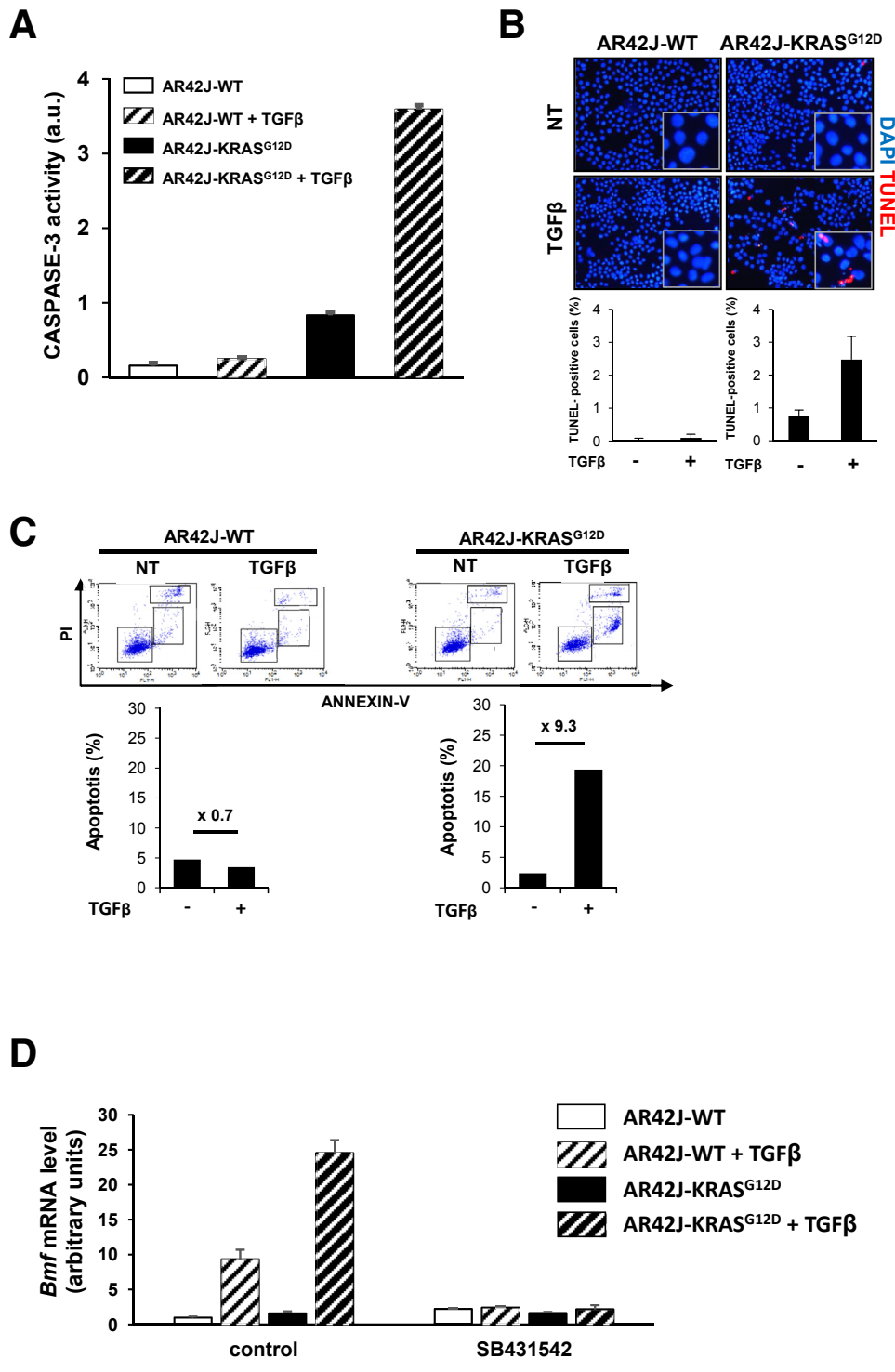


**Figure 1.** KRAS<sup>G12D</sup> potentiates TGFβ-mediated cell growth inhibition of AR42J rat pancreatic acinar cells. (A) Immunoblot of RAS-GTP and total RAS on AR42J-WT and AR42J-KRAS<sup>G12D</sup> protein extracts. (B) Phase microscopy of AR42J-WT and AR42J-KRAS<sup>G12D</sup> cells 48 hours after TGFβ treatment. Insets represent higher magnifications fields. Scale bar, 50 μm/L. NT, untreated. \*Apoptotic cells. (C) Cell count of AR42J-WT and AR42J-KRAS<sup>G12D</sup> cells at indicated times after TGFβ treatment. Representative experiment performed in duplicate (means ± standard deviation) is shown. (D) Immunoblot of SMAD proteins after 2-hour TGFβ treatment.

obtained [E2A-Cre; LSL-TβRI<sup>CA</sup>] mice (Figure 4), strongly suggesting that the expression of TβRI<sup>CA</sup> at an early stage of development was embryonically or prenatally lethal. To restrict TGFβ gain-of-function to the whole organism of mice postpartum, we generated [Rosa-Cre<sup>ERT2</sup>; LSL-TβRI<sup>CA</sup>] mice that were subsequently treated with tamoxifen to induce ubiquitous Cre-mediated recombination, the Rosa-26 locus being active in all adult lineages (Figure 5A). All [Rosa-Cre<sup>ERT2</sup>; LSL-TβRI<sup>CA</sup>] mice ( $n = 4$ ) injected with tamoxifen at the age of 7–10 weeks were euthanized 4 or 5 days after treatment because of the rapid onset of a highly

detrimental phenotype, whereas all of the wild-type mice survived ( $n = 5$ ) (Figure 5B). Histologic examination of the internal organs revealed that the pancreas was the most impaired organ, with many apoptotic figures (Figure 5C), clearly indicating a deleterious effect of TβRI activation in the pancreas, which could explain the severe phenotype of these animals. To test this hypothesis, we expressed TβRI<sup>CA</sup> in all of the pancreatic epithelial lineages by crossing [LSL-TβRI<sup>CA</sup>] (R) and [Pdx1-Cre] (C) mice,<sup>40</sup> which drives Cre recombinase expression in embryonic progenitors (at E8.5) of all pancreatic epithelial



lineages (Figure 5D). Histologic analysis revealed that [*Pdx1-Cre; LSL-T $\beta$ RI<sup>CA</sup>*] embryos (CR) presented pancreatic defects characterized by a massive reduction in the number of mature acinar cells (hematoxylin-eosin staining) along with abnormally abundant ductal structures (shown by CK19 expression) (Figure 5E). No obvious

defect in the endocrine compartment was observed (using INSULIN staining as a marker) (Figure 5E). These latter results show that pancreatic activation of TGF $\beta$  signaling at an early stage of development affects normal pancreatic development by impacting the acinar cell compartment.

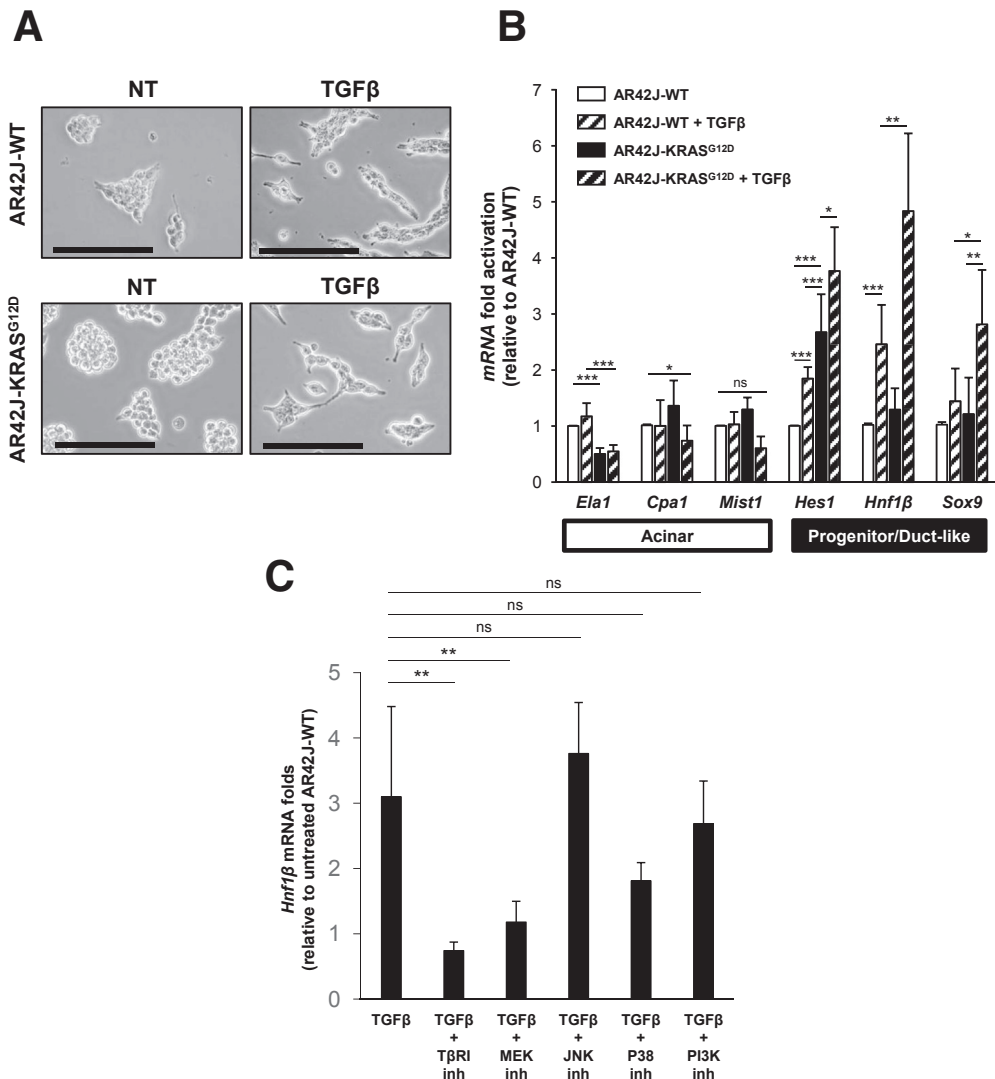


**Figure 3. KRAS<sup>G12D</sup> and TGFβ cooperate to activate dedifferentiation of AR42J rat acinar cells.** (A) High-magnification microscopy of rat acinar cells (AR42J). Phase-contrast microscopy of AR42J-WT and AR42J-KRAS<sup>G12D</sup> cells treated or not with TGFβ for 48 hours. NT, untreated. Scale bars, 100 μm. (B) RT-qPCR of acinar (*Ela-1*, *Cpa1*, *Mist1*), progenitor (*Hnf1β*, *Hes1*), and ductal (*Sox9*) markers after 48-hour TGFβ treatment. For each condition, expression is represented as mean ± standard deviation of at least 3 independent experiments. Statistical analyses were performed by using Mann-Whitney test: \*P < .05, \*\*P < .01, \*\*\*P < .001. Non-significant (ns) if P > .05. (C) Signaling pathways involved in TGFβ-induced *Hnf1β* mRNA activation. AR42J-WT cells were cultured in presence of TGFβ along with different kinase inhibitors (inh) of canonical and non-canonical TGFβ pathways: TβRI inh, SB431542; MEK inh, U0126 monoethanolate; JNK inh, JNK-IN-8; P38 inh, SB2023580; PI3K inh, LY294002. *Hnf1β* mRNA was detected by RT-qPCR after 48-hour treatment. For each condition, folds are represented as mean ± standard deviation of at least 3 independent experiments. Statistical analyses were performed by using Mann-Whitney U test: \*\*P < .01. Nonsignificant (ns) if P > .05.

### Inducible TβRI<sup>CA</sup> Expression in Pancreatic Acinar Cells After Birth Results in SMAD Pathway Activation

To circumvent the afore-mentioned embryonic developmental defects, we investigated the effects of *TβRI<sup>CA</sup>* expression starting after birth. To that end, we used the tamoxifen-inducible Pft1a-Cre<sup>ERT2</sup> mouse allele (C<sup>ER</sup>),<sup>5</sup> which limits the expression of Cre recombinase to adult acinar cells (Figure 6A). Mice were injected with tamoxifen at 5 weeks of age. Excision of the floxed transcriptional Stop in the pancreas of C<sup>ER</sup>R(+TAM) mice was validated by PCR on genomic DNA (Figure 6B).

RT-qPCR experiments revealed a significant enrichment in *TβRI<sup>CA</sup>* mRNA in C<sup>ER</sup>R(+TAM) pancreata compared with R pancreata, which was correlated with upregulation of the TGFβ-target gene *Serpine-1* (Figure 6C). Immunoprecipitation assays and Western blot analyses revealed a marked accumulation of P-SMAD2 in the pancreata of C<sup>ER</sup>R(+TAM) compared with wild-type mice (Figure 6D) (as expected the level of total SMAD2 in the lysates or in the immunoprecipitates did not differ between wild-type and C<sup>ER</sup>R(+TAM) mice). Next, we ascertained that the expression of the *TβRI<sup>CA</sup>* transgene was restricted to the pancreatic acinar compartment by performing

	# litters	# pups	# pups/litter	WT	[E2a-Cre]	[LSL-T $\beta$ R $^{CA}$ ]	[E2a-Cre; LSL-T $\beta$ R $^{CA}$ ]
[E2a-Cre $^{+/+}$ ] x [LSL-T $\beta$ R $^{CA}$ ]	4	18	4.5		18		0
[E2a-Cre $^{+/-}$ ] x [LSL-T $\beta$ R $^{CA}$ ]	5	29	5.8	10	7	12	0
			Fisher's exact test	ns	ns	ns	*

**Figure 4.** Early activation of T $\beta$ RI $^{CA}$  during mouse development is embryonically lethal. [E2A-Cre $^{+/+}$ ] or [E2A-Cre $^{+/-}$ ] mice were crossed with [LSL-T $\beta$ R $^{CA}$ ] (R) mice. Total number of litters, pups, and offspring genotype distribution are presented. Fisher's exact test was performed to statistically confirm absence of [E2A-Cre $^{+/-}$ ; LSL-T $\beta$ R $^{CA}$ ] mice. Nonsignificant (ns),  $P > .05$ ; \* $P < .05$ .

RNAscope (Figure 6E). It is worth noting that 100% of the acinar cells expressed the transgene, and that transgene expression was not observed in other lineages (ducts and islets). In addition, the detection of Smad7 mRNA by RNAscope suggested that the canonical TGF $\beta$ -SMAD pathway was activated *in vivo* in the presence of T $\beta$ RI $^{CA}$ . These results clearly indicate that the conditional T $\beta$ RI $^{CA}$  transgene is restricted to pancreatic epithelial cells on tamoxifen treatment and is correlated with the activation of the SMAD pathway *in vivo*.

#### Acinar-to-Ductal Metaplasia in Response to T $\beta$ RI $^{CA}$ Expression

Activating mutations of KRAS (eg, KRAS $G12D$ ) are found in >90% of human PDAs and are sufficient to trigger carcinogenesis when targeted in mice.<sup>49</sup> We generated mice expressing T $\beta$ RI $^{CA}$  (R) and Kras $G12D$  (K) transgenes either alone or in combination under the control of Pft1a-Cre $^{ERT2}$  (C $^{ER}$ ), and we performed histologic analyses of pancreata collected at different time points after tamoxifen injection (3 days, 3 weeks, 2 months, and 6 months). As early as 3 days after tamoxifen treatment (Figure 7A), C $^{ER}$ R(+TAM) and C $^{ER}$ KR(+TAM) pancreata presented a severe reduction in the acinar compartment associated with increased apoptosis (Figure 7B; H&E, black arrowheads; TUNEL). C $^{ER}$ K(+TAM) were normal and C $^{ER}$ KR(+TAM) undistinguishable from C $^{ER}$ R(+TAM) pancreata. Amylase is a marker of acinar cells, whereas CK19 and SOX9 are ductal markers. SOX9 is also an early positive regulator of ADM. Interestingly, we observed that C $^{ER}$ R(+TAM) and C $^{ER}$ KR(+TAM) pancreata displayed double-positive CK19 $^+$ /amylase $^+$  or SOX9 $^+$ /amylase $^+$  acinar cells (Figure 7B, immunofluorescence, white arrowheads), a feature of acinar cells undergoing early ADM reprogramming to form ductal-like structures.<sup>50</sup> These "ducts" consisted of simple cuboidal epithelial cells and were characterized by the expression of stemness markers and ductal markers. These double-positive acinar cells (CK19 $^+$ /amylase $^+$ , SOX9 $^+$ /amylase $^+$ ) most likely correspond to a regenerative process accompanying acinar cell loss. Three weeks after tamoxifen treatment (Figure 8), C $^{ER}$ K(+TAM) pancreata were still normal. However, compared with the analysis performed 3 days after tamoxifen injection, we observed a drastic loss in the acinar compartment (amylase $^+$ ), concomitantly with a large increase in the number of duct-like structures (CK19 $^+$ ), when T $\beta$ RI $^{CA}$  was expressed (C $^{ER}$ R(+TAM)), independently of oncogenic KRAS activation (eg, KRAS $G12D$ ).

#### Tumorigenesis Induced by KRAS $G12D$ Is Enhanced by T $\beta$ RI $^{CA}$

Two and 6 months after tamoxifen treatment (Figure 9A and B), we observed in C $^{ER}$ R(+TAM) pancreata a massive loss of acinar tissue replaced by adipose tissue, a phenomenon known as acinar fatty infiltration (AFI). In C $^{ER}$ K(+TAM) pancreata, PanINs and ADM lesions were clearly distinguishable without clear evidence of AFI. Interestingly, C $^{ER}$ KR(+TAM) double mutant pancreata presented both AFI and PanINs. Precise quantitative and qualitative analysis of epithelial lesions (Figure 9C) revealed at 2 months a 3-fold increase in the number of PanIN1 in C $^{ER}$ KR(+TAM) compared with C $^{ER}$ K(+TAM) and the absence of PanIN2 in C $^{ER}$ K(+TAM), whereas these lesions were detectable in C $^{ER}$ KR(+TAM). At 6 months the analysis showed the presence of PanIN3/PDA only in C $^{ER}$ KR(+TAM) (absence in C $^{ER}$ K(+TAM)), with three-fourths of C $^{ER}$ KR(+TAM) mice developing PDA compared with 0 of 5 C $^{ER}$ K(+TAM) mice (Fisher's exact test,  $P = .0476$ ; data not shown).

In double mutants, a strong desmoplastic reaction associated with a drastic reduction of the acinar compartment was observed at 2 and 6 months. Immunohistochemistry analysis of pancreata at 2 months and 6 months after tamoxifen induction confirmed the ductal nature of the lesions and demonstrated that T $\beta$ RI $^{CA}$  expression in C $^{ER}$ R(+TAM) mice does not further affect endocrine islets compared with C $^{ER}$ K(+TAM), which we have previously shown to present disorganized islets architecture<sup>51</sup> (Figure 10).

Our results demonstrate that in adult mice (1) activation of TGF $\beta$  signaling induces ADM by disrupting acinar cell homeostasis, leading to a drastic increase in the number of ductal structures at the expense of acinar structures; and (2) activation of TGF $\beta$  signaling in combination with oncogenic KRAS activation leads to the early onset of pre-neoplastic lesions that can naturally evolve toward high-grade/locally invasive lesions.

#### Discussion

Tumorigenesis can be divided into 3 consecutive steps. The priming stage corresponds to biological processes (such as cellular stress, inflammation, dedifferentiation) that predispose normal cells to further transformation by creating a propitious cellular state or microenvironment. The initiation stage is represented by all genetic and epigenetic events sufficient for the acquisition of the transformed phenotype

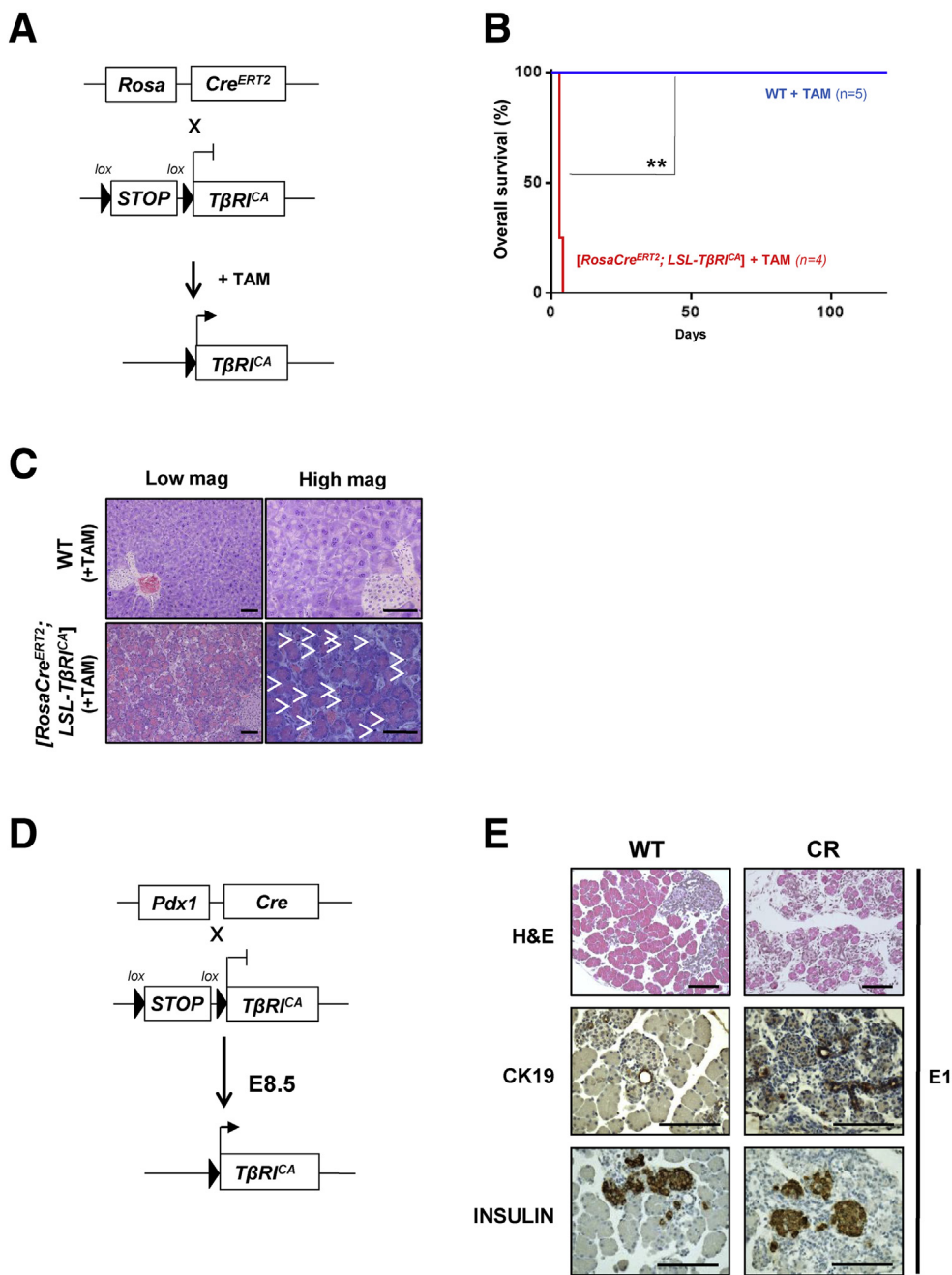
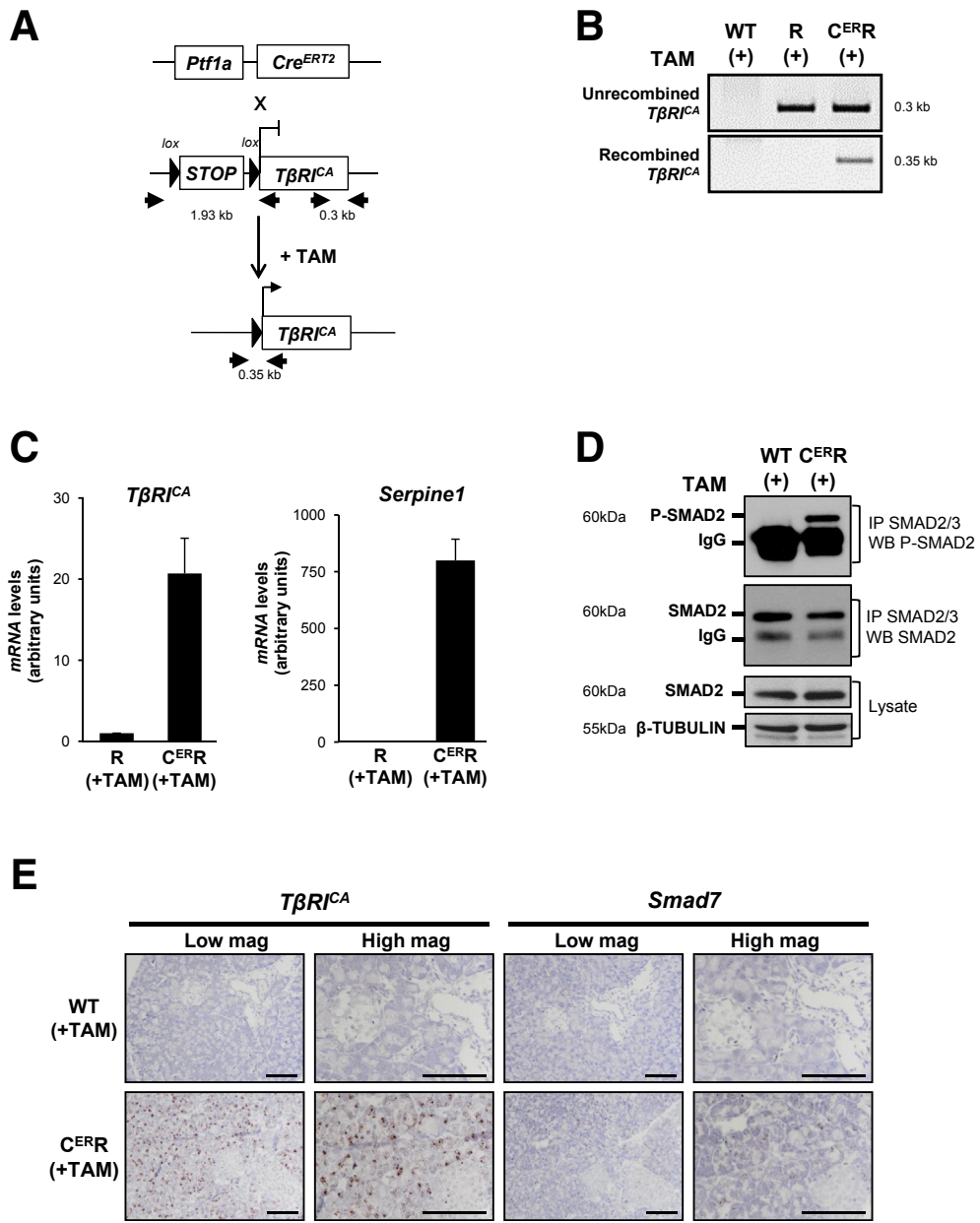


**Figure 5. Expression of T $\beta$ RI $^{CA}$  in mouse embryo compromises development of acinar compartment.** (A) Breeding strategy to target T $\beta$ RI $^{CA}$  expression in whole adult body by using tamoxifen-inducible Rosa26-Cre $^{ERT2}$  allele. (B) Overall survival (Kaplan-Meier analysis) of wild-type (WT) and [Rosa26-Cre $^{ERT2}$ ; LSL-T $\beta$ RI $^{CA}$ ] mice after tamoxifen injection. Log-rank (Mantel-Cox) test. \*\*P = .0047. (C) Histology of pancreata prepared from WT and [Rosa26-Cre $^{ERT2}$ ; LSL-T $\beta$ RI $^{CA}$ ] mice 5 days after tamoxifen injection. White arrows, apoptotic cells. Scale bars, 200  $\mu$ m. (D) Breeding strategy to target T $\beta$ RI $^{CA}$  expression in all epithelial pancreatic lineages from embryonic day 8.5 (E8.5) by using Pdx1-Cre allele. (E) Histology of pancreata prepared from WT and [Pdx1-Cre; LSL-T $\beta$ RI $^{CA}$ ] (CR) E19.5 embryos. Scale bars, 200  $\mu$ m. mag, magnification; TAM, tamoxifen.

(such as KRAS activating mutations). The progression/metastatic stage is characterized by mechanisms conferring aggressiveness and invasive properties to cancer cells (such as inactivation of TP53 or SMAD4 tumor suppressors). Bioactive TGF $\beta$ , which is found in normal and pathologic pancreas tissues, plays a crucial role in both normal tissue homeostasis and pancreatic diseases. The TGF $\beta$  paradox in cancer consists in the observation that TGF $\beta$  behaves either as a tumor suppressor or as a tumor promoter depending on the cellular context, especially in the 3 above-described stages. The studies conducted so far to address the multi-faceted role of TGF $\beta$  in pancreatic cancer *in vivo* mostly relied on loss-of-function approaches (receptor inactivation,

SMAD inactivation) and ligand gain-of-function (effect is not restricted to cancer cells). These strategies did not provide a clear answer as to the precise role of TGF $\beta$  signaling in pancreatic epithelial cells. In the present study, we developed a conditional and inducible TGF $\beta$  gain-of-function mouse model expressing a constitutively active type I TGF $\beta$  receptor (T $\beta$ RI $^{CA}$ ) in the pancreas. We demonstrated that cell-autonomous expression of T $\beta$ RI $^{CA}$  in the epithelial pancreatic compartment could severely compromise acinar cell homeostasis by inducing early ADM reprogramming. This phenotype was associated with the activation of both a proapoptotic program and a ductal-like differentiation program. Lately, the predominant role of necrosis (a

**Figure 6.** Inducible  $T\beta R^{CA}$  expression in pancreatic acinar cells after birth results in SMAD pathway activation *in vivo*. (A) Breeding strategy to express  $T\beta R^{CA}$  after birth in pancreatic acinar cells by using tamoxifen-inducible  $Pft1a$ -Cre $^{ERT2}$  allele. Black arrows represent genotyping primers. Sizes of expected fragments are shown. (B) PCR on genomic DNA to assess excision of STOP signal in C $^{ERR}$  mice after tamoxifen injection. (C) RT-qPCR of  $T\beta R^{CA}$  and Serpine-1 on total RNA from pancreata prepared from mice treated with tamoxifen. Expression level in R mice was arbitrarily set at 1 (mean  $\pm$  standard deviation; 2 independent experiments). (D) Immunoprecipitation of SMAD2/3 and Western blot analysis of P-SMAD2 (phospho-SMAD2) and total SMAD2. Total lysate was assessed for  $\beta$ -tubulin and SMAD2. (E) RNAscope detection of  $T\beta R^{CA}$  and Smad7 mRNA on pancreatic sections from WT and C $^{ERR}$  mice. Scale bars, 100  $\mu$ m. (A–E): WT, wild-type; R, [LSL- $T\beta R^{CA}$ ]; C $^{ERR}$ , [Pft1a-Cre $^{ERT2}$ ; LSL- $T\beta R^{CA}$ ]. mag, magnification; TAM, tamoxifen.

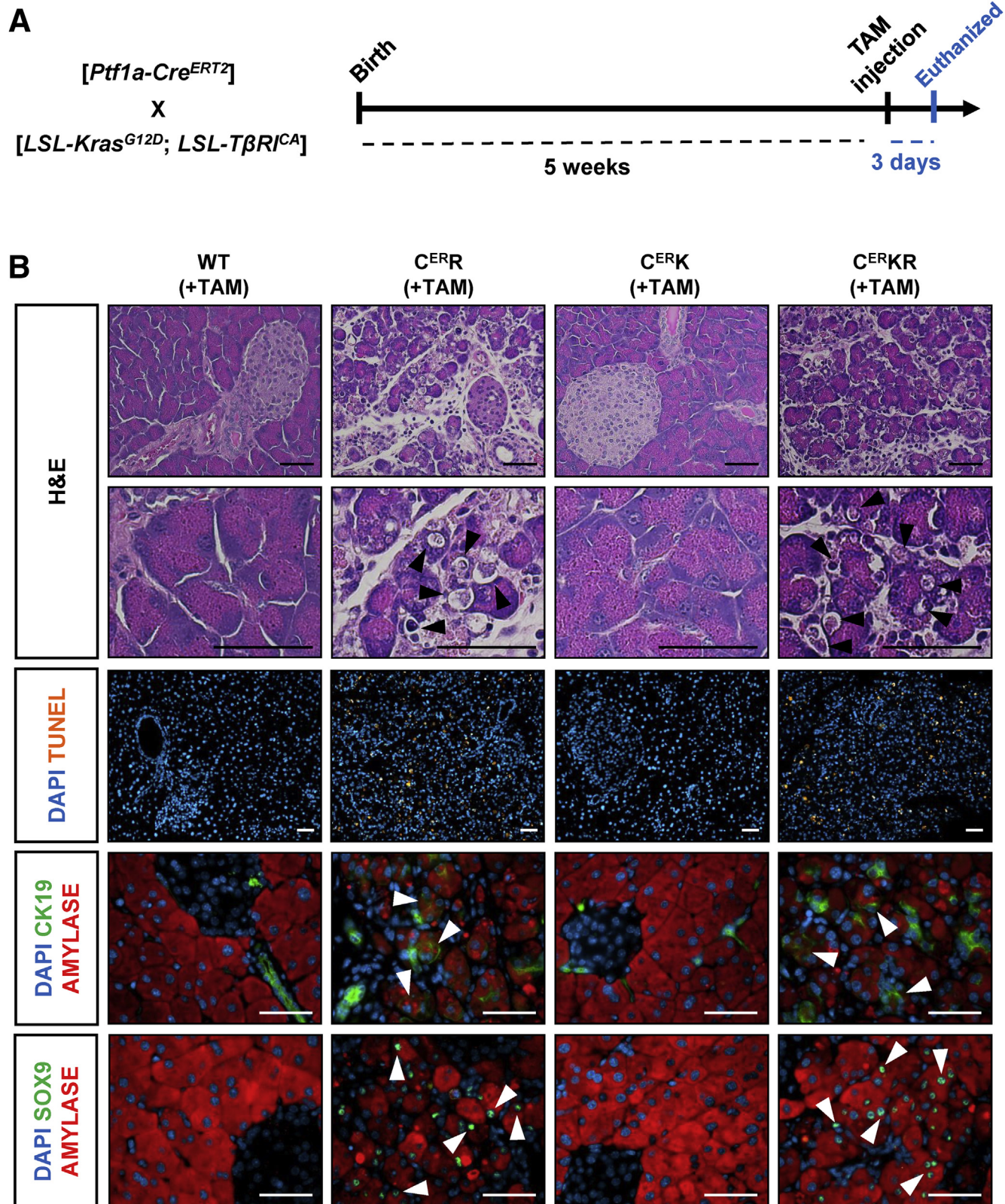


programmed form of necrosis death) in acinar cell death was reported in severe experimental mouse pancreatitis.<sup>52</sup> We also demonstrated that in the presence of mutated KRAS $G12D$ , TGF $\beta$ -induced ADM reprogramming facilitates the onset of PanINs. This work represents a demonstration that the activation of cell-autonomous TGF $\beta$  signaling compromises pancreatic acinar cell identity and eventually potentiates KRAS $G12D$ -driven tumor initiation.

#### Cell-autonomous Transforming Growth Factor Beta Activation Induces Acinar-to-Ductal Metaplasia Reprogramming

Three days after  $T\beta R^{CA}$  induction in adult mouse pancreatic acinar cells, we observed a drastic reduction in

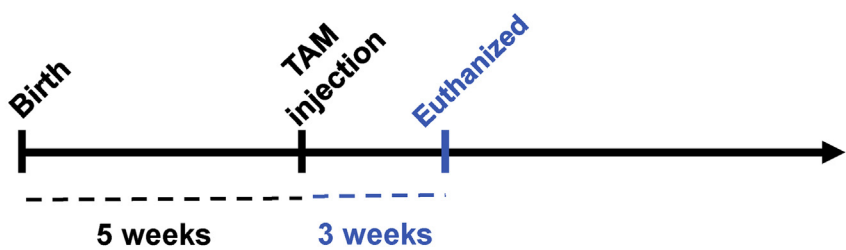
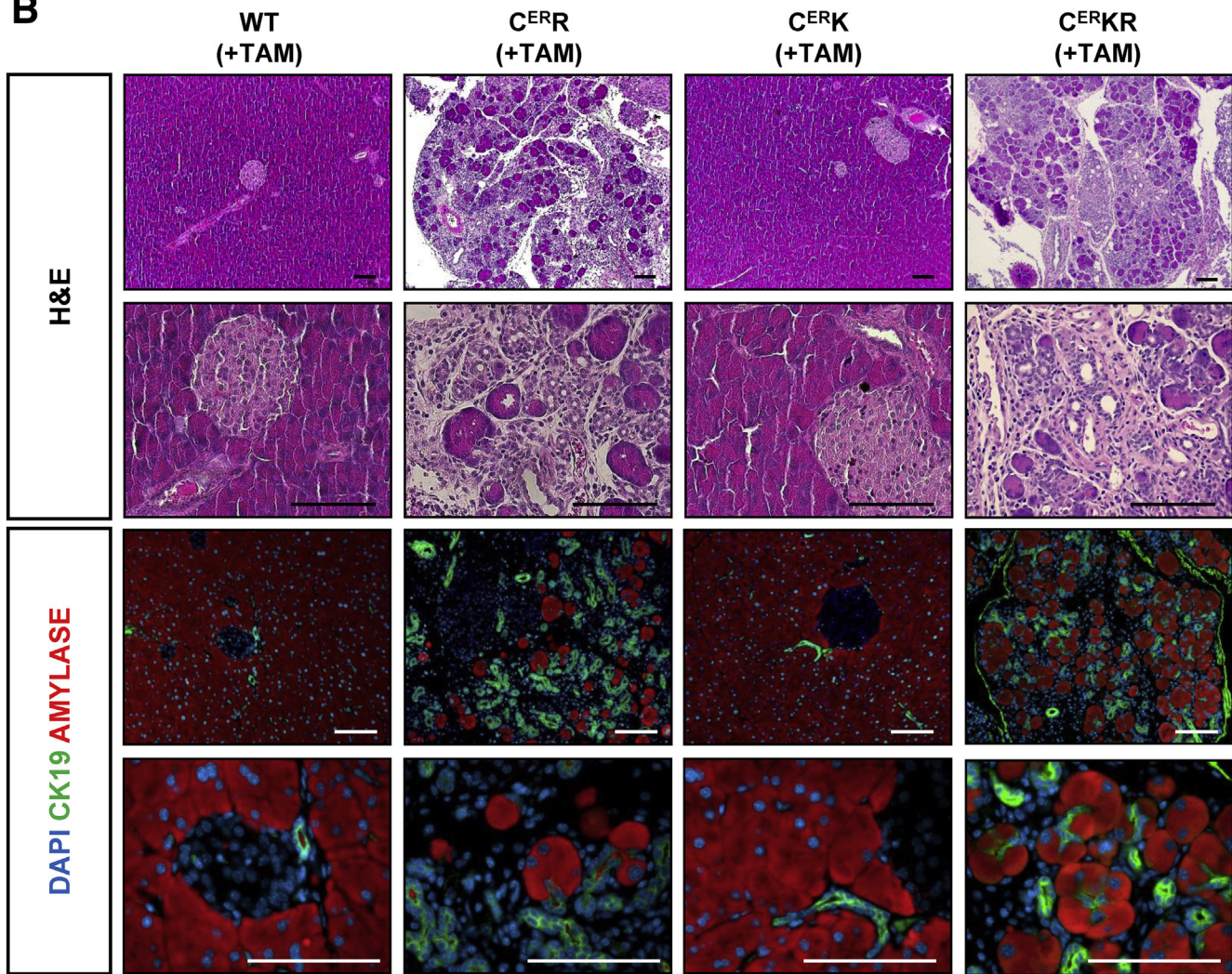
acinar tissue as attested by decreased amylase expression in the pancreata of mice expressing the transgene. This observation corroborates previous studies, which reported a repressive role for TGF $\beta$  on the fate of acinar cells. Indeed, it was demonstrated that TGF $\beta$  could inhibit the formation of acinar tissue *ex vivo* in cultures of pancreatic embryonic buds.<sup>53</sup> *In vivo*, by using a transgenic mouse model expressing a type II TGF $\beta$  dominant-negative mutant receptor under the regulation of the metallothionein 1 (*Mt1*) promoter, TGF $\beta$  was shown to be essential for the maintenance of the acinar compartment homeostasis.<sup>54</sup> In the present study, we observed that targeted activation of TGF $\beta$  signaling in acinar cells *in vivo* efficiently compromised acinar identity. At the microscopic level, we observed that the loss of acinar tissue was associated with massive



**Figure 7.** *T $\beta$ R<sup>CA</sup>* expression in acinar cells induces apoptosis and ductal-like differentiation 3 days after induction. (A) Diagram of experimental design for 5-week-old mice injected with tamoxifen and euthanized 3 days later. (B) H&E staining, TUNEL assay, and immunofluorescence of amylase, CK19, and SOX9. Black arrowheads, apoptotic cells; white arrowheads, CK19/amylose and SOX9/amylose double-positive cells; WT, wild-type; [*Ptf1a-Cre<sup>ERT2</sup>*; *LSL-T $\beta$ R<sup>CA</sup>*], C<sup>ER</sup>R; [*Ptf1a-Cre<sup>ERT2</sup>*; *LSL-Kras<sup>G12D</sup>*], C<sup>ER</sup>K; [*Ptf1a-Cre<sup>ERT2</sup>*; *LSL-T $\beta$ R<sup>CA</sup>*; *LSL-Kras<sup>G12D</sup>*], C<sup>ER</sup>KR. TAM, tamoxifen. Scale bars, 50  $\mu$ m.

**A**

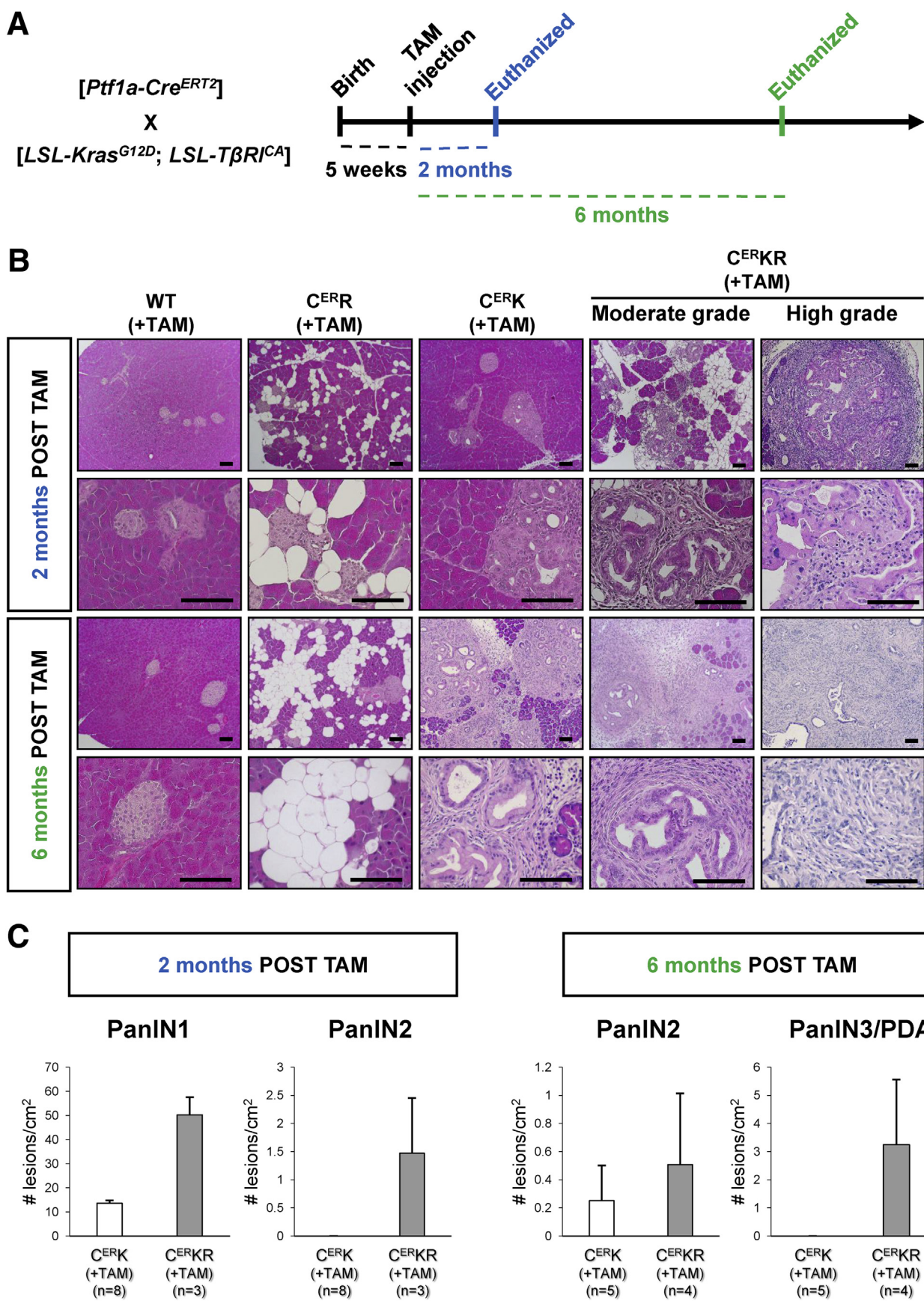
$[Ptf1a-Cre^{ERT2}]$   
X  
 $[LSL-Kras^{G12D}; LSL-T\beta RI^{CA}]$

**B**

**Figure 8.**  $T\beta RI^{CA}$  expression in acinar cells leads to regenerative ADM 3 weeks after induction. (A) Diagram of experimental design for 5-week-old mice injected with tamoxifen and euthanized 3 weeks later. (B) H&E staining and immunofluorescence of amylase and CK19. WT, wild-type;  $[Ptf1a-Cre^{ERT2}; LSL-T\beta RI^{CA}]$ ,  $C^{ER}R$ ;  $[Ptf1a-Cre^{ERT2}; LSL-Kras^{G12D}]$ ,  $C^{ER}K$ ;  $[Ptf1a-Cre^{ERT2}; LSL-T\beta RI^{CA}; LSL-Kras^{G12D}]$ ,  $C^{ER}KR$ . TAM, tamoxifen. Scale bars, 100  $\mu$ m.

apoptosis and with the appearance of new highly abundant ductal structures of small diameter. This phenotype is reminiscent of ADM, a process involved in pancreas replenishment after tissue injury.<sup>1,6,11</sup> During this process and as observed in the model presented here, the acinar cells are reprogrammed into a ductal-like cell population,

displaying features of progenitor cells, with the ability to regenerate the different lineages in the injured pancreas. Recently, Liu et al.<sup>55</sup> have shown that TGF $\beta$  could convert primary human acinar cells to ductal-like cells *in vitro*, which corroborates our current *in vivo* demonstration that TGF $\beta$  induces ADM. Although the signals triggering ADM



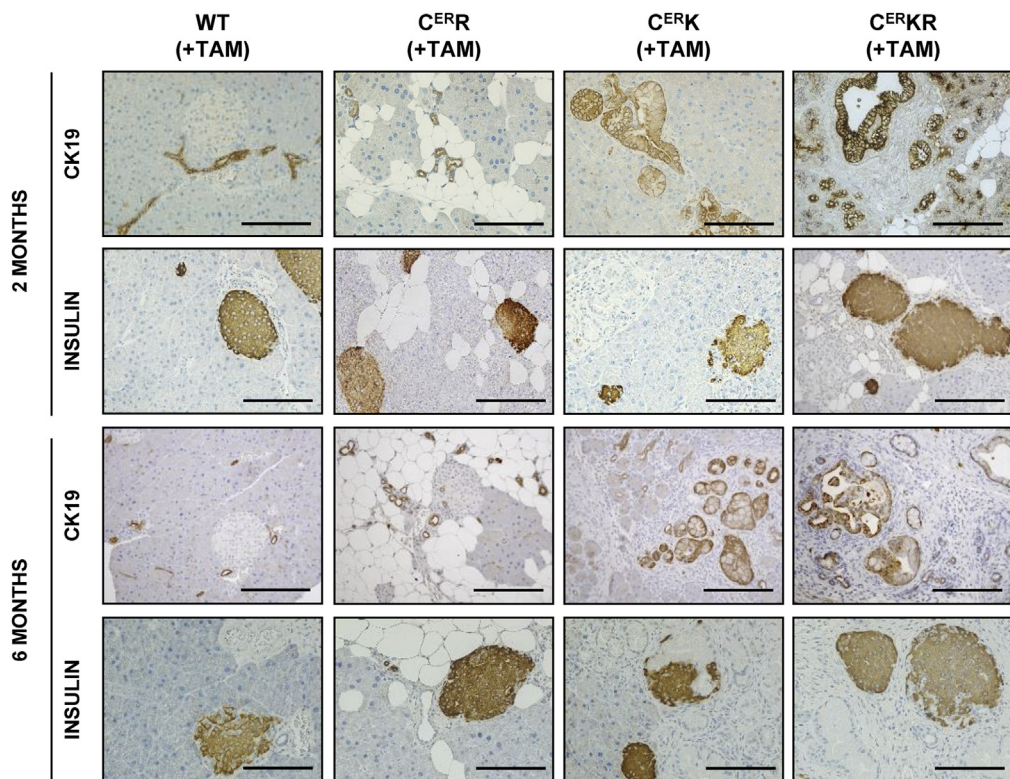


**Figure 10. KRAS<sup>G12D</sup> and TGF $\beta$  activation cooperate to accelerate pancreatic tumorigenesis without affecting endocrine compartment.**

Immunohistochemical detection of CK19 and INSULIN in mice of indicated genotypes 2 and 6 months after tamoxifen induction. [Pft1a-Cre<sup>ERT2</sup>; LSL-T $\beta$ R $I^{CA}$ ] (C<sup>ERT</sup>R); [Pft1a-Cre<sup>ERT2</sup>; LSL-Kras<sup>G12D</sup>] (C<sup>ERK</sup>); [Pft1a-Cre<sup>ERT2</sup>; LSL-T $\beta$ R $I^{CA}$ ; LSL-Kras<sup>G12D</sup>] (C<sup>ERKR</sup>). Scale bars, 200  $\mu$ m.

*in vivo* are poorly known, we demonstrate herein that TGF $\beta$  signaling activation is one of these signals.

#### Acinar-to-Ductal Metaplasia Reprogramming Induced by Transforming Growth Factor Beta Activation Facilitates KRAS<sup>G12D</sup>-mediated Carcinogenesis

ADM has largely been documented to represent the first step in pancreatic tumor development by providing a suitable surrounding for the malignant transformation of cells in response to oncogene-driven mutations such as KRAS<sup>G12D</sup>.<sup>12</sup> Here we report a significant increase in both the number and the grade of PanIN lesions in the pancreas of mice expressing both T $\beta$ R $I^{CA}$  and Kras<sup>G12D</sup> transgenes in comparison with age-matched KRAS<sup>G12D</sup> mice. PanINs were never observed in the presence of T $\beta$ R $I^{CA}$  alone. This observation supports the idea that KRAS<sup>G12D</sup> generates a persistent ADM (known as for acinar-to-ductal reprogramming<sup>56</sup>), facilitating the subsequent onset of PanINs. Active TGF $\beta$  thus appears to be crucial to potentiate KRAS<sup>G12D</sup> transforming properties through its capacity to confer a ductal-like phenotype to acinar cells that possess progenitor properties and that are more sensitive to transformation. It

is worth underlining that the phenotype we observed in the pancreas of T $\beta$ R $I^{CA}$  mice resembles that of pancreatitis, a pathology predisposing to PDA.<sup>57</sup> In aging mice we observed that ADM was resolved by AFI, which represents the normal evolution of chronic pancreatitis when the inflammatory stress ceases. Pancreatitis characterized by ADM has also been reported to be tightly dependent on TGF $\beta$  activation. Indeed, it was shown by others that inhibition of TGF $\beta$  in different mouse models, by using a dominant-negative type II TGF $\beta$  receptor,<sup>58-60</sup> by overexpressing the inhibitory SMAD7,<sup>61</sup> or by using halofuginone to inhibit TGF $\beta$ -induced collagen deposition,<sup>62</sup> could compromise cerulein-induced pancreatitis. Pancreatitis has also been shown to be reversible in the absence of activated KRAS and irreversible in the presence of activated KRAS,<sup>63</sup> demonstrating that KRAS<sup>G12D</sup> is able to harness the pancreatitis phenotype to facilitate the development of PanINs. The presence of activated KRAS would then prevent spontaneous resorption of the phenotype, driving cells toward persistent ADM and PanINs. Our findings, together with these previous studies, demonstrate that TGF $\beta$  activation in the pancreas induces ADM, providing a propitious environment, with features reminiscent of pancreatitis, for the onset of KRAS<sup>G12D</sup>-induced PanINs. Hence, cell-autonomous activation of TGF $\beta$

**Figure 9. (See previous page). T $\beta$ R $I^{CA}$  expression in acinar cells accelerates KRAS<sup>G12D</sup>-induced tumorigenesis several months after induction.** (A) Diagram of experimental design representing 5-week-old mice injected with tamoxifen and euthanized 2 or 6 months later. (B) H&E staining. WT, wild-type; [Pft1a-Cre<sup>ERT</sup>; LSL-T $\beta$ R $I^{CA}$ ], C<sup>ERT</sup>R; [Pft1a-Cre<sup>ERT2</sup>; LSL-Kras<sup>G12D</sup>], C<sup>ERK</sup>; [Pft1a-Cre<sup>ERT2</sup>; LSL-T $\beta$ R $I^{CA}$ ; LSL-Kras<sup>G12D</sup>], C<sup>ERKR</sup>. Scale bars, 100  $\mu$ m. (C) Quantification of pancreatic epithelial lesions at different grades and observed in C<sup>ERK</sup> and C<sup>ERKR</sup> pancreata 2 months and 6 months after TAM injection. TAM, tamoxifen.

signaling in pancreatic acinar cells may represent a crucial step in pancreatitis, which is also known to predispose to PDA, thus providing a physiopathologic relevance for the results described in the present study.

### **Simultaneous Transforming Growth Factor Beta Signaling and KRAS Activation Cooperate to Induce Apoptosis and Ductal Reprogramming of Acinar Cells**

We demonstrated *in vitro* and *in vivo* that the simultaneous activation of TGF $\beta$  and KRAS could cooperate to induce apoptosis and ductal reprogramming of acinar cells, two cellular events classically observed in pancreatic ADM.<sup>7</sup> Importantly, in the tamoxifen-inducible model, 100% of pancreatic epithelial cells expressed the *T $\beta$ RI<sup>CA</sup>* transgene *in vivo*, thus indicating that the deleterious phenotype observed in the presence of the *KRAS<sup>G12D</sup>* transgene resulted from a cell-autonomous functional interaction. Although our observations indicate that TGF $\beta$  activation induces direct ADM reprogramming, the mechanisms dictating cell fate, *i.e.*, apoptotic death *versus* survival associated with the acquisition of an ADM phenotype, remain to be uncovered. Indeed, the mechanisms that allow a proportion of acinar cells to escape apoptosis and pursue their route toward ADM remain to be identified. As suggested by a recent study, the fate of pancreatic cancer cells is tightly controlled by factors downstream of TGF $\beta$  (SNAIL and SOX4).<sup>64</sup> David et al<sup>64</sup> showed that TGF $\beta$ -induced EMT resulted in apoptosis activation and tumor suppressive activity. Hence, in the transformed pancreas, TGF $\beta$ -induced apoptosis reduces the number of cancer cells, thus substantiating its tumor suppressive effect at this stage, whereas in the normal pancreas (the present work), TGF $\beta$  induced apoptosis and promotes ADM, thereby proving its oncogenic effect. Whether this model proposed by David et al can be transposed to untransformed cells to study tumor initiation needs to be tested.

On the basis of the use of AR42J rat acinar cells stably expressing KRAS<sup>G12D</sup> and treated with TGF $\beta$ , we were able to show that KRAS activation sensitized acinar cells to both TGF $\beta$ -induced apoptosis and dedifferentiation. At the molecular level, we evidenced in this model a cooperative effect of both pathways to modulate the expression of *Hnf1 $\beta$* , *Sox9*, and *Hes1*. The combination of these 3 transcription factors is a hallmark of the formation of progenitor cells during development,<sup>3</sup> which is in accordance with the well-documented role of TGF $\beta$  as a promoter of stemness.<sup>65,66</sup> Indeed, SOX9 and HNF1 $\beta$  are the first transcription factors that commit endoderm cells to pancreatic progenitors during organogenesis.<sup>5</sup> They are markers of the ductal tree, re-expressed during ADM.<sup>3,14</sup> Moreover, the adult SOX9 has been shown to be a master positive regulator of the ADM process.<sup>56</sup> Indeed, the ectopic expression of SOX9 in acinar cells activates the expression of ductal markers and increases KRAS<sup>G12D</sup>-induced ADM, and conversely, inactivation of *Sox9* in KRAS<sup>G12D</sup>-expressing adult acinar cells compromises the onset of PanINs, confirming its critical role in the transition toward a ductal phenotype.<sup>56</sup> In the present study, we reported that the *in vivo* co-expression of *T $\beta$ RI<sup>CA</sup>*

and KRAS<sup>G12D</sup> was able to induce the onset of amylase/SOX9 double-positive cells. This feature is known to be associated with the regenerative process after acinar cell loss, stemming from double-positive cells for acinar and ductal markers. The precise role of SOX9 in this model remains to be explored and whether *Hes1* and *Hnf1 $\beta$*  are direct transcriptional targets of SMAD proteins. How KRAS<sup>G12D</sup> potentiates their activation is currently under investigation in our laboratory.

### **Physiopathologic Relevance and Therapeutic Implications**

Our observation that TGF $\beta$  behaves as a tumor promoter may seem paradoxical in light of other studies showing that inactivation of TGF $\beta$  signaling by inactivating *Smad4* or *T $\beta$ RII* accelerates the progression of KRAS<sup>G12D</sup>-induced lesions.<sup>67-72</sup> This is most likely a consequence of both the gain-of-function approach we used and the stage at which TGF $\beta$  signaling was impaired. Indeed, in our model through its capacity to induce ADM, activation of TGF $\beta$  signaling resulted in an increased KRAS<sup>G12D</sup>-induced tumor initiation. This can be explained by the effect of TGF $\beta$  on the priming stage of tumor progression by committing acinar cells to an ADM differentiation program favorable to transformation. In contrast, *T $\beta$ RII* or *Smad4* homozygous deletions facilitate the progression of KRAS<sup>G12D</sup>-induced preexisting PanINs. This observation is consistent with the loss of *SMAD4* at late stages and widespread metastatic human diseases.<sup>73,74</sup> Furthermore, we recently demonstrated that the activation of TGF $\beta$  signaling was sufficient to induce the onset of ovarian tumors, strongly supporting our current findings that this signaling pathway plays an active role in promoting tumor initiation.<sup>36</sup> Overall, this work sheds new light on another level of complexity for the dual role of TGF $\beta$  as a tumor promoter and suppressor.

TGF $\beta$  or components of its signaling pathway are being extensively evaluated as a potential therapeutic target, as attested by the compelling preclinical and encouraging clinical studies.<sup>75</sup> As a consequence of its dual role in cancer, deciphering TGF $\beta$ -related functional processes is a prerequisite to develop efficient anti-TGF $\beta$  therapies. Understanding the first steps of pancreatic tumorigenesis is necessary to determine how pancreatic tumor cells acquire plasticity. Such an effort may provide new therapeutic strategies aimed at restoring a normal differentiated state. An example of a successful differentiation therapy was observed in acute promyelocytic leukemia,<sup>76,77</sup> characterized by the accumulation of incompletely differentiated leukemic cells, which could be forced to fully differentiate on treatment with all-transretinoic acid. More recently, Fitamant et al<sup>78</sup> provided proof-of-concept for differentiation therapy in solid tumors by deleting *Yap1* in hepatocellular carcinoma, which present features of progenitor cells. In this context, unveiling the specific effects of TGF $\beta$  at different stages of tumorigenesis may lead to innovative therapeutic strategies aimed at restoring acinar differentiation and, therefore, at decreasing the deleterious onset of cellular plasticity. Defining the molecular mechanisms

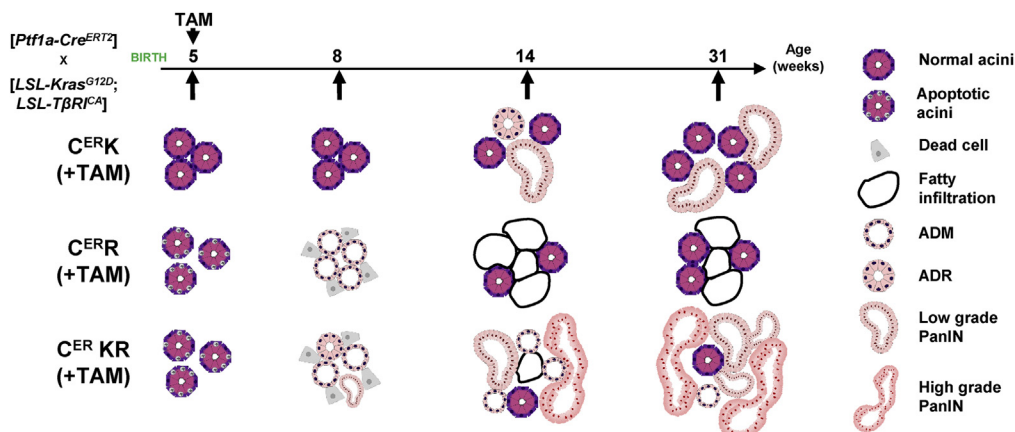


**Figure 11. Schematic diagram showing effect of TGF $\beta$  signaling activation (alone or in combination with KRAS $G^{12D}$ ) on pancreatic acinar compartment.** A few days after tamoxifen induction, T $\beta$ RI $CA$  induces acinar cell apoptosis and subsequent regenerative metaplasia (ADM). In aging mice, ADM is overcome and replaced by ADR. KRAS $G^{12D}$  activation alone induces ADM and PanINs several months after induction. When T $\beta$ RI $CA$  and KRAS $G^{12D}$  are simultaneously induced, PanINs develop much earlier. In the context of T $\beta$ RI $CA$ -induced ADM, KRAS $G^{12D}$  induces regenerative cells to undergo the ADM>ADR>PanIN sequence (ADR, acinar-to-ductal reprogramming). Hence, TGF $\beta$  signaling activation enhances the properties of KRAS $G^{12D}$  through its capacity to prime a suitable surrounding for transformation. TAM, tamoxifen. [Ptf1a-Cre $ERT^2$ ; LSL-T $\beta$ RI $CA$ ], C $ER$ K; [Ptf1a-Cre $ERT^2$ ; LSL-T $\beta$ RI $CA$ ; LSL-Kras $G^{12D}$ ], C $ER$ R; [Ptf1a-Cre $ERT^2$ ; LSL-Kras $G^{12D}$ ], C $ER$ KR. TAM, tamoxifen. WT, wild-type.

underlying the initiation of pancreatic cancer is highly relevant for the development of early detection markers and new therapies. Indeed, inhibition of TGF $\beta$  may represent a therapeutic strategy for impeding ductal reprogramming of acinar cells to prevent the initiation of PDA in high-risk patients (hereditary syndrome or chronic pancreatitis).

In conclusion, the present study demonstrates that TGF $\beta$  is an ADM inducer, facilitating the development of pancreatic neoplastic lesions in a KRAS $G^{12D}$ -dependent context. According to the activated state of KRAS and TGF $\beta$  signaling, we propose an integrated and dynamic model for pancreatic cancer initiation; TGF $\beta$  activation is not sufficient to induce PanINs, and KRAS $G^{12D}$  is poorly efficient at inducing ADM. However, when combined, TGF $\beta$  induces ADM and provides a propitious setting for KRAS $G^{12D}$ -induced transformation (Figure 11). Defining the molecular mechanisms underlying the initiation of pancreatic cancer is highly relevant for the development of early detection markers and of potentially novel treatments.

## References

- Puri S, Folias AE, Hebrok M. Plasticity and dedifferentiation within the pancreas: development, homeostasis, and disease. *Cell Stem Cell* 2015;16:18–31.
- Jorgensen MC, Ahnfelt-Ronne J, Hald J, Madsen OD, Serup P, Hecksher-Sorensen J. An illustrated review of early pancreas development in the mouse. *Endocr Rev* 2007;28:685–705.
- Shih HP, Wang A, Sander M. Pancreas organogenesis: from lineage determination to morphogenesis. *Annu Rev Cell Dev Biol* 2013;29:81–105.
- Pan FC, Wright C. Pancreas organogenesis: from bud to plexus to gland. *Dev Dyn* 2011;240:530–565.
- Pan FC, Bankaitis ED, Boyer D, Xu X, van de Casteele M, Magnuson MA, Heimberg H, Wright CV. Spatiotemporal patterns of multipotentiality in Ptf1a-expressing cells during pancreas organogenesis and injury-induced facultative restoration. *Development* 2013;140:751–764.
- Ziv O, Glaser B, Dor Y. The plastic pancreas. *Dev Cell* 2013;26:3–7.
- Murtaugh LC, Keefe MD. Regeneration and repair of the exocrine pancreas. *Annu Rev Physiol* 2015;77:229–249.
- Beer RL, Parsons MJ, Rovira M. Centroacinar cells: at the center of pancreas regeneration. *Dev Biol* 2016;413:8–15.
- Bailey JM, DelGiorno KE, Crawford HC. The secret origins and surprising fates of pancreas tumors. *Carcinogenesis* 2014;35:1436–1440.
- Abel EV, Simeone DM. Biology and clinical applications of pancreatic cancer stem cells. *Gastroenterology* 2013;144:1241–1248.
- Stanger BZ, Hebrok M. Control of cell identity in pancreas development and regeneration. *Gastroenterology* 2013;144:1170–1179.
- Mills JC, Sansom OJ. Reserve stem cells: differentiated cells reprogram to fuel repair, metaplasia, and neoplasia in the adult gastrointestinal tract. *Sci Signal* 2015;8:re8.
- Jensen JN, Cameron E, Garay MV, Starkey TW, Gianani R, Jensen J. Recapitulation of elements of embryonic development in adult mouse pancreatic regeneration. *Gastroenterology* 2005;128:728–741.
- Roy N, Hebrok M. Regulation of cellular identity in cancer. *Dev Cell* 2015;35:674–684.
- Macgregor-Das AM, Iacobuzio-Donahue CA. Molecular pathways in pancreatic carcinogenesis. *J Surg Oncol* 2013;107:8–14.
- Ryan DP, Hong TS, Bardeesy N. Pancreatic adenocarcinoma. *N Engl J Med* 2014;371:1039–1049.
- Hahn SA, Schutte M, Hoque AT, Moskaluk CA, da Costa LT, Rozenblum E, Weinstein CL, Fischer A, Yeo CJ, Hruban RH, Kern SE. DPC4, a candidate tumor

- suppressor gene at human chromosome 18q21.1. *Science* 1996;271:350–353.
18. Knudsen ES, O'Reilly EM, Brody JR, Witkiewicz AK. Genetic diversity of pancreatic ductal adenocarcinoma and opportunities for precision medicine. *Gastroenterology* 2016;150:48–63.
  19. Massague J. TGFbeta signalling in context. *Nat Rev Mol Cell Biol* 2012;13:616–630.
  20. Morikawa M, Deryck R, Miyazono K. TGF-beta and the TGF-beta family: context-dependent roles in cell and tissue physiology. *Cold Spring Harb Perspect Biol* 2016;8.
  21. Deryck R, Zhang YE. Smad-dependent and Smad-independent pathways in TGF-beta family signalling. *Nature* 2003;425:577–584.
  22. Principe DR, Doll JA, Bauer J, Jung B, Munshi HG, Bartholin L, Pasche B, Lee C, Grippo PJ. TGF-beta: duality of function between tumor prevention and carcinogenesis. *J Natl Cancer Inst* 2014;106:djt369.
  23. Bartholin L, Vincent DF, Valcourt U. TGF- $\beta$  as tumor suppressor: in vitro mechanistic aspects of growth inhibition. In: Moustakas A, Miyazawa K, eds. *TGF- $\beta$  in human disease*. Tokyo: Springer Japan, 2013: 113–138.
  24. Pickup M, Novitskiy S, Moses HL. The roles of TGFbeta in the tumour microenvironment. *Nat Rev Cancer* 2013; 13:788–799.
  25. Padua D, Massague J. Roles of TGFbeta in metastasis. *Cell Res* 2009;19:89–102.
  26. Ikushima H, Miyazono K. TGFbeta signalling: a complex web in cancer progression. *Nat Rev Cancer* 2010; 10:415–424.
  27. Bierie B, Moses HL. TGF-beta and cancer. *Cytokine Growth Factor Rev* 2006;17:29–40.
  28. Vincent DF, Kaniewski B, Powers SE, Havenar-Daughton C, Marie JC, Wotton D, Bartholin L. A rapid strategy to detect the recombined allele in LSL-TbetaRI(CA) transgenic mice. *Genesis* 2010;48:559–562.
  29. Bartholin L, Cyprian FS, Vincent D, Garcia CN, Martel S, Horvat B, Berthet C, Goddard-Léon S, Treilleux I, Rimokh R, Marie JC. Generation of mice with conditionally activated transforming growth factor beta signaling through the T $\beta$ RI/ALK5 receptor. *Genesis* 2008; 46:724–731.
  30. Ruiz AL, Soudja SM, Deceneux C, Lauvau G, Marie JC. NK1.1+ CD8+ T cells escape TGF-beta control and contribute to early microbial pathogen response. *Nat Commun* 2014;5:5150.
  31. McCarron MJ, Marie JC. TGF-beta prevents T follicular helper cell accumulation and B cell autoreactivity. *J Clin Invest* 2014;124:4375–4386.
  32. Havenar-Daughton C, Li S, Benlagha K, Marie JC. Development and function of murine RORgamma $+$  iNKT cells are under TGF-beta signaling control. *Blood* 2012;119:3486–3494.
  33. Viel S, Marcais A, Guimaraes FS, Loftus R, Rabilloud J, Grau M, Degouve S, Djebali S, Sanlaville A, Charrier E, Bienvenu J, Marie JC, Caux C, Marvel J, Town L, Huntington ND, Bartholin L, Finlay D, Smyth MJ, Walzer T. TGF-beta inhibits the activation and functions of NK cells by repressing the mTOR pathway. *Sci Signal* 2016;9:ra19.
  34. Viant C, Rankin LC, Girard-Madoux MJ, Seillet C, Shi W, Smyth MJ, Bartholin L, Walzer T, Huntington ND, Vivier E, Belz GT. Transforming growth factor-beta and Notch ligands act as opposing environmental cues in regulating the plasticity of type 3 innate lymphoid cells. *Sci Signal* 2016;9:ra46.
  35. Mohammed J, Beura LK, Bobr A, Astry B, Chicoine B, Kashem SW, Welty NE, Iggyarto BZ, Wijeyesinghe S, Thompson EA, Matte C, Bartholin L, Kaplan A, Sheppard D, Bridges AG, Shlomchik WD, Masopust D, Kaplan DH. Stromal cells control the epithelial residence of DCs and memory T cells by regulated activation of TGF-beta. *Nat Immunol* 2016;17:414–421.
  36. Gao Y, Vincent DF, Davis AJ, Sansom OJ, Bartholin L, Li Q. Constitutively active transforming growth factor beta receptor 1 in the mouse ovary promotes tumorigenesis. *Oncotarget* 2016.
  37. Gao Y, Duran S, Lydon JP, DeMayo FJ, Burghardt RC, Bayless KJ, Bartholin L, Li Q. Constitutive activation of transforming growth factor Beta receptor 1 in the mouse uterus impairs uterine morphology and function. *Biol Reprod* 2015;92:34.
  38. Hadjantonakis AK, Cox LL, Tam PP, Nagy A. An X-linked GFP transgene reveals unexpected paternal X-chromosome activity in trophoblastic giant cells of the mouse placenta. *Genesis* 2001;29:133–140.
  39. Jackson EL, Willis N, Mercer K, Bronson RT, Crowley D, Montoya R, Jacks T, Tuveson DA. Analysis of lung tumor initiation and progression using conditional expression of oncogenic K-ras. *Genes Development* 2001; 15:3243–3248.
  40. Gu G, Dubauskaite J, Melton DA. Direct evidence for the pancreatic lineage: NGN3+ cells are islet progenitors and are distinct from duct progenitors. *Development* 2002;129:2447–2457.
  41. Hameyer D, Loonstra A, Eshkind L, Schmitt S, Antunes C, Groen A, Bindels E, Jonkers J, Krimpenfort P, Meuwissen R, Rijswijk L, Bex A, Berns A, Bockamp E. Toxicity of ligand-dependent Cre recombinases and generation of a conditional Cre deleter mouse allowing mosaic recombination in peripheral tissues. *Physiol Genomics* 2007;31:32–41.
  42. Lakso M, Pichel JG, Gorman JR, Sauer B, Okamoto Y, Lee E, Alt FW, Westphal H. Efficient in vivo manipulation of mouse genomic sequences at the zygote stage. *Proc Natl Acad Sci U S A* 1996;93:5860–5865.
  43. Vincent DF, Yan KP, Treilleux I, Gay F, Arfi V, Kaniewski B, Marie JC, Lepinasse F, Martel S, Goddard-Leon S, Iovanna JL, Dubus P, Garcia S, Puisieux A, Rimokh R, Bardeesy N, Scoazec JY, Losson R, Bartholin L. Inactivation of TIF1gamma cooperates with Ras to induce cystic tumors of the pancreas. *PLoS Genet* 2009;5:e1000575.
  44. Vincent DF, Gout J, Chuvin N, Arfi V, Pommier RM, Bertolino P, Jonckheere N, Ripoche D, Kaniewski B, Martel S, Langlois JB, Goddard-Leon S, Colombe A, Janier M, Van Seuningen I, Losson R, Valcourt U, Treilleux I, Dubus P, Bardeesy N, Bartholin L. Tif1gamma

- suppresses murine pancreatic tumoral transformation by a smad4-independent pathway. *Am J Pathol* 2012; 180:2214–2221.
45. Longnecker DS, Lilja HS, French J, Kuhlmann E, Noll W. Transplantation of azaserine-induced carcinomas of pancreas in rats. *Cancer Lett* 1979;7:197–202.
  46. Jessop NW, Hay RJ. Characteristics of two rat pancreatic exocrine cell lines derived from transplantable tumors. *Vitro* 1980;16:212.
  47. Heldin C-H, Landström M, Moustakas A. Mechanism of TGF- $\beta$  signaling to growth arrest, apoptosis, and epithelial-mesenchymal transition. *Current Opinion in Cell Biology* 2009;21:166–176.
  48. Ramjaun AR, Tomlinson S, Eddaudia A, Downward J. Upregulation of two BH3-only proteins, Bmf and Bim, during TGF beta-induced apoptosis. *Oncogene* 2007; 26:970–981.
  49. Hingorani SR, Petricoin EF, Maitra A, Rajapakse V, King C, Jacobetz MA, Ross S, Conrads TP, Veenstra TD, Hitt BA, Kawaguchi Y, Johann D, Liotta LA, Crawford HC, Putt ME, Jacks T, Wright CV, Hruban RH, Lowy AM, Tuveson DA. Preinvasive and invasive ductal pancreatic cancer and its early detection in the mouse. *Cancer Cell* 2003;4:437–450.
  50. Zhu L, Shi G, Schmidt CM, Hruban RH, Koniczny SF. Acinar cells contribute to the molecular heterogeneity of pancreatic intraepithelial neoplasia. *Am J Pathol* 2007; 171:263–273.
  51. Gout J, Pommier RM, Vincent DF, Ripoche D, Goddard-Leon S, Colombe A, Treilleux I, Valcourt U, Tomasini R, Dufresne M, Bertolino P, Bartholin L. The conditional expression of KRAS G12D in mouse pancreas induces disorganization of endocrine islets prior the onset of ductal pre-cancerous lesions. *Pancreatology* 2013; 13:191–195.
  52. Louhimo J, Steer ML, Perides G. Necroptosis is an important severity determinant and potential therapeutic target in experimental severe pancreatitis. *Cell Mol Gastroenterol Hepatol* 2016;2:519–535.
  53. Sanvito F, Herrera PL, Huarte J, Nichols A, Montesano R, Orci L, Vassalli JD. TGF-beta 1 influences the relative development of the exocrine and endocrine pancreas in vitro. *Development* 1994;120:3451–3462.
  54. Bottlinger EP, Jakubczak JL, Roberts IS, Mumy M, Hemmati P, Bagnall K, Merlino G, Wakefield LM. Expression of a dominant-negative mutant TGF-beta type II receptor in transgenic mice reveals essential roles for TGF-beta in regulation of growth and differentiation in the exocrine pancreas. *Embo J* 1997; 16:2621–2633.
  55. Liu J, Akanuma N, Liu C, Naji A, Half GA, Washburn WK, Sun L, Wang P. TGF-beta1 promotes acinar to ductal metaplasia of human pancreatic acinar cells. *Sci Rep* 2016;6:30904.
  56. Kopp JL, von Figura G, Mayes E, Liu FF, Dubois CL, Morris JP, Pan FC, Akiyama H, Wright CV, Jensen K, Hebrok M, Sander M. Identification of Sox9-dependent acinar-to-ductal reprogramming as the principal mechanism for initiation of pancreatic ductal adenocarcinoma. *Cancer Cell* 2012;22:737–750.
  57. Duell EJ, Lucenteforte E, Olson SH, Bracci PM, Li D, Risch HA, Silverman DT, Ji BT, Gallinger S, Holly EA, Fontham EH, Maisonneuve P, Bueno-de-Mesquita HB, Ghadirian P, Kurtz RC, Ludwig E, Yu H, Lowenfels AB, Seminara D, Petersen GM, La Vecchia C, Boffetta P. Pancreatitis and pancreatic cancer risk: a pooled analysis in the International Pancreatic Cancer Case-Control Consortium (PanC4). *Ann Oncol* 2012; 23:2964–2970.
  58. Nagashio Y, Ueno H, Imamura M, Asaumi H, Watanabe S, Yamaguchi T, Taguchi M, Tashiro M, Otsuki M. Inhibition of transforming growth factor beta decreases pancreatic fibrosis and protects the pancreas against chronic injury in mice. *Lab Invest* 2004; 84:1610–1618.
  59. Yoo BM, Yeo M, Oh TY, Choi JH, Kim WW, Kim JH, Cho SW, Kim SJ, Hahm KB. Amelioration of pancreatic fibrosis in mice with defective TGF-beta signaling. *Pancreas* 2005;30:e71–e79.
  60. Wildi S, Kleeff J, Mayerle J, Zimmermann A, Bottlinger EP, Wakefield L, Buchler MW, Friess H, Korc M. Suppression of transforming growth factor beta signalling aborts caerulein induced pancreatitis and eliminates restricted stimulation at high caerulein concentrations. *Gut* 2007;56:685–692.
  61. He J, Sun X, Qian KQ, Liu X, Wang Z, Chen Y. Protection of cerulein-induced pancreatic fibrosis by pancreas-specific expression of Smad7. *Biochim Biophys Acta* 2009;1792:56–60.
  62. Zion O, Genin O, Kawada N, Yoshizato K, Roffe S, Nagler A, Iovanna JL, Halevy O, Pines M. Inhibition of transforming growth factor beta signaling by halofuginone as a modality for pancreas fibrosis prevention. *Pancreas* 2009;38:427–435.
  63. Morris JP, Wang SC, Hebrok M. KRAS, Hedgehog, Wnt and the twisted developmental biology of pancreatic ductal adenocarcinoma. *Nat Rev Cancer* 2010; 10:683–695.
  64. David CJ, Huang YH, Chen M, Su J, Zou Y, Bardeesy N, Iacobuzio-Donahue CA, Massague J. TGF-beta tumor suppression through a lethal EMT. *Cell* 2016; 164:1015–1030.
  65. Oshimori N, Fuchs E. The harmonies played by TGF-beta in stem cell biology. *Cell Stem Cell* 2012;11:751–764.
  66. Massague J, Xi Q. TGF-beta control of stem cell differentiation genes. *FEBS Lett* 2012;586:1953–1958.
  67. Bardeesy N, Cheng KH, Berger JH, Chu GC, Pahler J, Olson P, Hezel AF, Horner J, Lauwers GY, Hanahan D, DePinho RA. Smad4 is dispensable for normal pancreas development yet critical in progression and tumor biology of pancreas cancer. *Genes Dev* 2006; 20:3130–3146.
  68. Izeradjene K, Combs C, Best M, Gopinathan A, Wagner A, Grady WM, Deng CX, Hruban RH, Adsay NV, Tuveson DA, Hingorani SR. Kras(G12D) and Smad4/Dpc4 haploinsufficiency cooperate to induce mucinous cystic neoplasms and invasive adenocarcinoma of the pancreas. *Cancer Cell* 2007;11:229–243.
  69. Kojima K, Vickers SM, Adsay NV, Jhala NC, Kim HG, Schoeb TR, Grizzle WE, Klug CA. Inactivation of Smad4

- accelerates Kras(G12D)-mediated pancreatic neoplasia. *Cancer Res* 2007;67:8121–8130.
70. Whittle MC, Izeradjene K, Rani PG, Feng L, Carlson MA, DelGiorno KE, Wood LD, Goggins M, Hruban RH, Chang AE, Calses P, Thorsen SM, Hingorani SR. RUNX3 controls a metastatic switch in pancreatic ductal adenocarcinoma. *Cell* 2015;161:1345–1360.
  71. Ijichi H, Chytil A, Gorska AE, Akre ME, Fujitani Y, Fujitani S, Wright CV, Moses HL. Aggressive pancreatic ductal adenocarcinoma in mice caused by pancreas-specific blockade of transforming growth factor-beta signaling in cooperation with active Kras expression. *Genes Dev* 2006;20:3147–3160.
  72. Principe DR, DeCant B, Mascarinas E, Wayne EA, Diaz AM, Akagi N, Hwang R, Pasche B, Dawson DW, Fang D, Bentrem DJ, Munshi HG, Jung B, Grippo PJ. TGFbeta signaling in the pancreatic tumor microenvironment promotes fibrosis and immune evasion to facilitate tumorigenesis. *Cancer Res* 2016;76:2525–2539.
  73. Wilentz RE, Iacobuzio-Donahue CA, Argani P, McCarthy DM, Parsons JL, Yeo CJ, Kern SE, Hruban RH. Loss of expression of Dpc4 in pancreatic intraepithelial neoplasia: evidence that DPC4 inactivation occurs late in neoplastic progression. *Cancer Res* 2000;60:2002–2006.
  74. Yachida S, Iacobuzio-Donahue CA. Evolution and dynamics of pancreatic cancer progression. *Oncogene* 2013;32:5253–5260.
  75. Neuzillet C, de Gramont A, Tijeras-Raballand A, de Mestier L, Cros J, Faivre S, Raymond E. Perspectives of TGF-beta inhibition in pancreatic and hepatocellular carcinomas. *Oncotarget* 2014;5:78–94.
  76. Breitman TR, Selonick SE, Collins SJ. Induction of differentiation of the human promyelocytic leukemia cell line (HL-60) by retinoic acid. *Proc Natl Acad Sci U S A* 1980; 77:2936–2940.
  77. Breitman TR, Collins SJ, Keene BR. Terminal differentiation of human promyelocytic leukemic cells in primary culture in response to retinoic acid. *Blood* 1981; 57:1000–1004.
  78. Fitamant J, Kottakis F, Benhamouche S, Tian HS, Chuvin N, Parachoniak CA, Nagle JM, Perera RM, Lapouge M, Deshpande V, Zhu AX, Lai A, Min B, Hoshida Y, Avruch J, Sia D, Camprecios G, McClatchey AI, Llovet JM, Morrissey D, Raj L, Bardeesy N. YAP inhibition restores hepatocyte differentiation in advanced HCC, leading to tumor regression. *Cell Rep* 2015.

Received December 9, 2016. Accepted May 25, 2017.

#### Correspondence

Address correspondence to: Laurent Bartholin, PhD, Centre de Recherche en Cancérologie de Lyon (CRCL), Inserm U1052, CNRS 5286, Université Claude Bernard Lyon 1, 69008, Lyon, France. e-mail: laurent.bartholin@lyon.unicancer.fr; fax: +33 (0)4 69 96 68 26.

#### Acknowledgments

The authors thank Dr Christophe Vanbelle for expert analyses in microscopy; the specific pathogen-free animal facility platform AniCan, ALECs-SPF facility and the Laboratoire des Modèles Tumoraux platform for animal care; the research and scientific services at the CRUK Beatson Institute in general; the laboratory of Dr Hingorani at the Fred Hutchinson Cancer Research Center for the help they provided during the revisions; and Christopher Wright for sharing the Ptf1a-Cre<sup>ERT2</sup> mice with us.

#### Author Contributions

Study concept and design were performed by NC, DFV, RMP, LBA, and LB. Acquisition of data was performed by NC, DFV, RMP, LBA, Jo.G, KY, CC, VC, ER, BK, SM, and CC. Analysis and interpretation of data were performed by NC, DFV, RMP, LBA, IT, VR, AC, OJS, UV, SS, PD, and LB. Drafting of the manuscript was performed by NC, DFV, and LB. Critical revision of the manuscript for important intellectual content was performed by NC, DFV, RMP, VR, AC, JM, Ju.G, OJS, UV, SS, PD, and LB. SS, LB and OJS obtained funding. Technical support was performed by SGL, AC, JV, NG, CC, JV, ES, and IG. LB supervised the study.

#### Conflicts of interest

The authors disclose no conflicts.

#### Funding

Supported by the Association pour la Recherche sur le Cancer (JG, DFV, and BK salaries), the Centre Léon Bérard (SM and CK salaries), the Ministère de l'Enseignement Supérieur et de la Recherche of France (DFV, RMP, and ER fellowships), by the Ligue Nationale Contre le Cancer (VC, LA, and LBA fellowships), from the Ecole Normale Supérieure of Lyon (NC fellowship), and by Stem Cells Arabia (KY salary). LB is supported by an Avenir grant (Inserm), an INCA grant, Ligue grants (Rhône, Haute-Savoie), and an ARC grant. SS is supported by a Ligue grant (Ardèche). OJS is supported by a Cancer Research UK core grant (A21139) and an ERC Starting grant (311301). DFV is supported by an ERC Starting grant (311301).